Optics and Fluid Dynamics Department annual progress report for 1994

Hanson, Steen Grüner; Lading, Lars; Lynov, Jens-Peter; Michelsen, Poul

Publication date:
1995

Document Version
Publisher's PDF, also known as Version of record

RISØ

Risø-R-793(EN)

Optics and Fluid Dynamics Department Annual Progress Report for 1994

Edited by S.G. Hanson, L. Lading, J.P. Lynov, and P. Michelsen

Risø National Laboratory, Roskilde, Denmark
January 1995

Optics and Fluid Dynamics Department Annual Progress Report for 1994

Risø-R-793(EN)

Edited by S.G. Hanson, L. Lading, J.P. Lynov, and P. Michelsen

Risø National Laboratory, Roskilde, Denmark
January 1995

Abstract Research in the Optics and Fluid Dynamics Department is performed within the following two programme areas: optics and continuum physics. In optics the activities are within (a) optical materials and electromagnetic propagation, (b) diagnostics and sensors, and (c) information processing. In continuum physics the activities are (a) nonlinear dynamics and (b) computer physics. The activities are supported by several EU programmes, including EURATOM, by research councils, and by industry. A special activity is the implementation of pellet injectors for fusion research. A summary of activities in 1994 is presented.

ISBN 87-550-2044-5
ISSN 0106-2840
ISSN 0906-1797

Grafisk Service · Risø · 1995

Contents

1 Introduction

The department performs basic and applied research within optics and continuum physics. The scope is understanding of physical phenomena as well as development of materials and systems for specific applications. The activities are often performed in collaboration with other research groups or industry. The training of students at a graduate level is an integral part of the activities and so is the dissemination of results to research and industry. The work is of importance for the understanding of the dynamics of fluids and plasmas, as well as for the understanding of optical diagnostic systems and new optical materials. Several results are exploited by industry.

The motivation for the combination of optics, fluid dynamics, and plasma physics is that most of the activities lie within what can be called continuum physics; only in some of the work on materials and photon statistics is a discrete atomised structure invoked. In addition, optical methods are applied to fluid and plasma diagnostics.

The work described in this report falls within the following categories:

- *Optical materials and electromagnetic propagation* are concentrated on nonlinear phenomena, storage materials, propagation and scattering, and laser ablation.
- *Diagnostics and sensors* for probing the dynamics of physical systems. Diffractive optics is often an essential part of the systems considered.
- *Information processing*, both electronic and optical, for pattern recognition and illumination with structured light in industrial systems.
- *Nonlinear dynamics* is concentrated on the understanding of nonlinear dynamic processes in fluids and fusion plasmas in close collaboration with computer physics.
- *Computer physics* which here is the application of spectral models to highly nonlinear distributed systems.
- *Pellet injection* systems have been developed and are delivered to fusion research laboratories.

Of major results in 1994 can be mentioned:

- The development of multidomain spectral codes that allow for the use of spectral models in connection with complex geometries.
- A new algorithm for the calculation of pressure fields based on spectral methods.
- Industrial collaboration concerning the verification of a novel particle image velocimetry system.
- The application of bacteriorhodopsin as an active medium for optical information processing.
- The demonstration of a new type of subharmonics in a photorefractive media that contradicts established models.
- Concepts for integrated optoelectronic sensors based on a combination of waveguide and diffractive structures.

2 Optics

2.1 Introduction

During the last decades the field of optics has steadily evolved to include optical materials, laser-based sensors, and optical processing - to mention a few. Consequently, the scientific foundation includes chemistry, electromagnetic field theory, and theory on stochastic processes. The outcome may enhance scientific knowledge but can also provide the basis for industrial products.

The work carried out in the Optics Section is diversified with a common denominator being future applications. Three major branches have been subject to investigations. The first, and largest, effort has been made within the field of optical materials, especially with bacteriorhodopsin and optically active polyesters, where the nonlinear properties have been of special interest. New architectures for optical processing and data storage appear as the scientific work in this field progresses. Nonlinear optical properties are observed and described in photorefractive crystals with special respect to measurement and description of the appearance of subharmonics. Laser ablation of materials is not only important as a tool for stoichiometrically conserved deposition of thin films. The target material will display surface relief structures reflecting the intensity distribution of the incident light. Besides, the interaction between the strong incident field and the substrate may convey detailed information on the material.

Optical diagnostics constitutes the second branch of interest for the Optics Section. The embedding of complex optical structures in one diffractive structure may bring about a means for designing and producing new optical sensors with a broader range of applications. Not only will the fabrication of the optical parts of the sensor systems be considerably simplified, but the lack of constraints in the design process will facilitate the implementation of new optical sensor systems. The theoretical description of the interaction of laser light with rough surfaces is based on stochastic processes. This description has been employed as well for the description of interaction between electromagnetic fields and surface waves in the ocean.

Processing of 2D structures with electronic processors has been the third and a vital part of the work in the Optics Section. Pattern recognition and feature tracking by electronically implemented neural networks constitute a robust scheme which can be implemented for supervised as well as for unsupervised learning. Three European programmes have been undertaken within this area during the period. All optical processing of 2D data has attractive features which have been the focus of rigorous attention. The scope of this field has been changed to try to combine the benefits of optical processing with the versatility of the electronic computer to prosper from the superiority of each technique.

2.2 Optical Materials

2.2.1 Side Chain Azo Polyesters for Optical Storage

(C. Holme, E. Rasmussen, P.S. Ramanujam, J. Stubager, S. Hvilsted*, M. Pedersen* (*Solid State Physics Department, Risø), F. Andruzzi+, P.L. Magagnini+ (+University of Pisa, Italy), I. Zebger[1], C. Kulinna[1], and H.W. Siesler[1] ([1]University of Essen, Germany))

In an ongoing project on side chain azo polyesters exhibiting permanent local changes in refractive index due to trans-cis isomerisation, the physics of optical

storage is being examined in detail. This system of polyesters has been shown to present a flexible architecture with several adjustable design parameters, such as the length of methylene sequence in the polyester main chain, the length of the flexible methylene spacers in the side chain, and the molar mass of the polyester. Each parameter has been demonstrated to affect the behaviour of the thin polyester films under irradiation by light from an argon ion laser[1]. We have made a detailed investigation of the implications due to a change in the length of the flexible spacer and that of the acidic constituent of the main chain for optical storage through measurements of the optical anisotropy. The side chains discussed here contain 6, 8, and 10 methylene spacers and the main chain contains 10 and 12 methylene groups.

The films have been produced by spin-coating on glass substrates 20 mg of the polyesters in 300 microlitres chloroform or toluene. The films are not preoriented. The time-dependent measurements of the optically induced anisotropy on the polyester films have been performed with the setup shown in Fig. 1, consisting of a HeNe laser at 633 nm and an argon ion laser at 488 nm. The vertically polarised beam from the argon ion laser is used as pump inducing the anisotropy and a very low-power HeNe laser beam polarised at 45° is used to probe the induced anisotropy. A Wollaston prism is used to split the HeNe beam after passing through the film into two components, one with polarisation parallel to the initial polarisation ($I_{\parallel}$), and one with polarisation perpendicular to the initial polarisation ($I_{\perp}$). It is shown that the transmission through the films depends on the laser intensity and that the polyesters with shorter flexible spacers respond more readily to low irradiation intensities. The effect of the film temperature during the pumping and probing cycles is being examined in detail in order to reveal the effect of the liquid crystallinity.

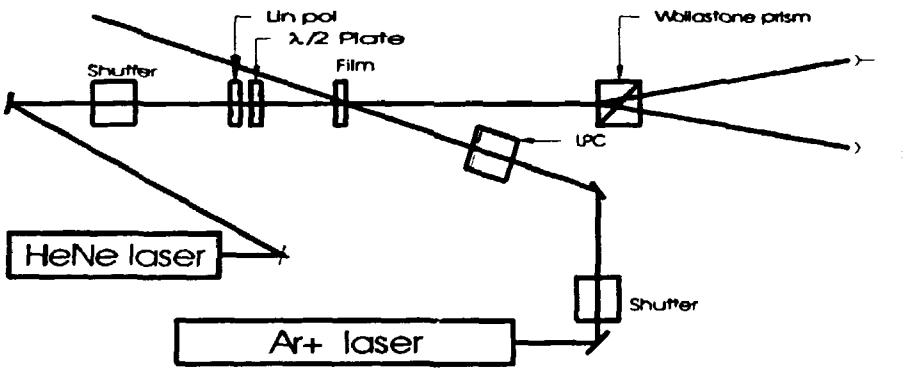

Figure 1. Experimental setup to measure optical anisotropy.

Both laser-induced anisotropy and holographic storage have been investigated in substituted polyesters (cyano, nitro, methoxy and unsubstituted)[2-4]. These investigations have been carried out at 413 and 488 nm. The highest efficiency obtained at 413 nm is about $2\text{-}3\times10^{-3}$ for the cyano and unsubstituted azobenzenes. Much higher efficiency is obtained at 488 nm albeit at higher incident intensities. Up to 13% efficiency has been obtained for the cyano at this wavelength. The poor efficiency at 413 nm is attributable to two reasons: (1) The absorption at 413 nm is three times as high as at 488 nm; this leads to the formation of absorption gratings whose efficiency is much less than that of pure phase gratings. (2) Since the absorption is larger, the light is probably getting absorbed within the first few nanometers of the film, rather than penetrating the entire depth. Thus, a large part of the azochromophores is probably not utilised. In general, the nitro

and methoxy substituents seem to give much lower diffraction efficiency. These findings are in agreement with the FTIR measurements. This is remarkable as one might expect that chromophores with higher dipole moments might provide higher mobility when interacting with light. However, the above results show that dipole moments may not be an important parameter as far as higher efficiency is concerned.

One of the most interesting physical aspects of the optical storage in these polyesters is that the storage is permanent in the polyesters with 12 methylene groups in the main chain even though the glass transition temperature is around 20° C. Through an investigation of the UV-Vis spectra, it has been shown that the lifetimes of the cis states in these polyesters are only of the order of three hours. A HeNe laser beam has been shown to induce backtransition to the trans states within the lifetimes of the cis states, resulting in a biphotonic process[5]. These results have been confirmed through polarised Fourier transform IR spectroscopy. It is surmised that the crystallinity of the main and side chains has important roles to play in the permanent storage of information. Investigations are being carried out with an atomic force microscope in order to confirm this hypothesis.

Computer-generated holograms and text have been directly recorded on side chain liquid polyester films. A HeCd laser, with an output of the order of 10 mW is used for recording. The laser beam is linearly polarised. After passing through an acousto-optic modulator (Bragg cell) the beam is collimated, and after passing through several optical components it is focused on the polyester film by a microscope objective mounted on a ten kg turnwheel (Fig. 2). The polyester film

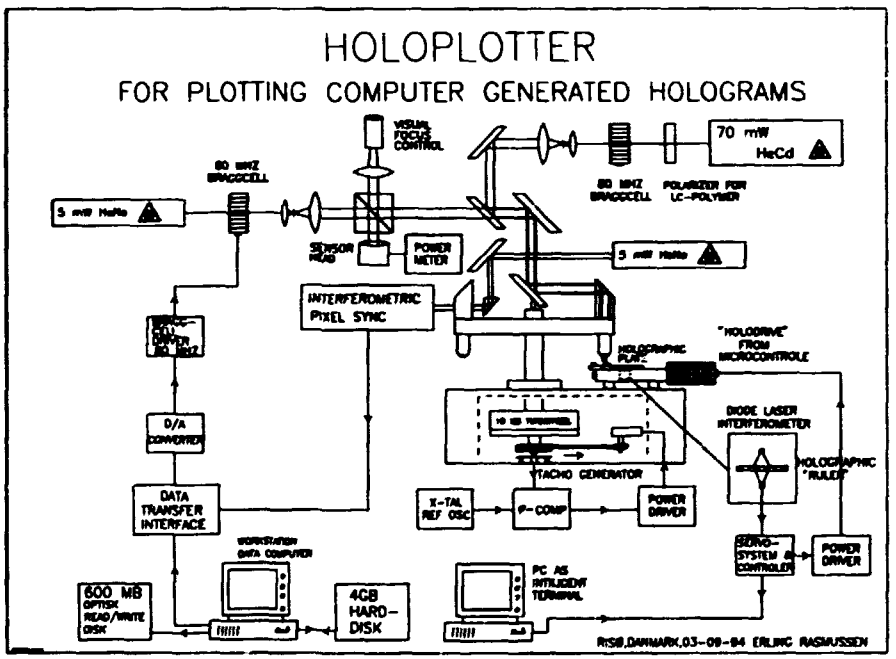

Figure 2. Holoplotter.

(holographic plate in figure) is mounted on a linear translator (holodrive) capable of making linear translations in steps of 100 nm. The turnwheel is driven by a precise quartz crystal oscillator in order to keep the revolving speed of the turnwheel highly constant. As the turnwheel rotates, the laser beam would scribe a line on the holographic plate. The holodrive translates the holographic plate constantly, so that the information is inscribed in the form of parallel displaced circular arcs

of constant radius on the holographic plate. The acousto-optic modulator serves to amplitude-modulate the laser beam in an analogue manner, controlled by a hardware-software correction table for the nonlinearity in the modulator, thus enabling a recording of several grey tones. The optical pattern, be it a diffraction pattern or text to be recorded on the film, is calculated by a workstation data computer and is used to turn the acousto-optic modulator on and off. The resolution of the system is at the moment about 300 lines/mm and this can probably be improved to about 500 lines/mm. Examples of computer-generated patterns are shown in Fig. 3.

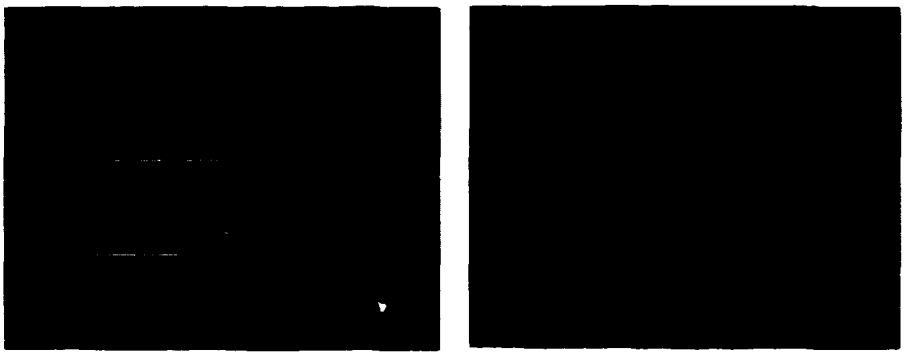

Figure 3. Examples of computer-generated patterns.

This work is supported by the Brite-Euram II project (contract no. BRE 2.CT93.-0449).

1) Ramanujam, P.S., Andruzzi, F., and Hvilsted, S. (1995). Optical Review **1**, 3.
2) Hvilsted, S., Pedersen, M., Ramanujam, P.S., and Andruzzi, F. (1994). Poster presented at 5th European Polymer Federation, Symposium on Polymeric Materials, Basel, Switzerland.
3) Zebger, I., Kulinna, Ch., Siesler, H.W., Andruzzi, F., Pedersen, M., Ramanujam, P.S., and Hvilsted, S. (1994). Poster presented at 11th European Symposium on Polymer Spectroscopy, Valladolid, Spain.
4) Pedersen, M., Hvilsted, S., Andruzzi, F., and Ramanujam, P.S. (1994). Poster presented at Nordiske Polymerdage, Copenhagen, Denmark.
5) Kulinna, Ch., Zebger, I., Hvilsted, S., Ramanujam, P.S., and Siesler, H.W. (1994). Macromol. Symp. **83**, 169.

2.2.2 Nonlinear Optical Effects in Bacteriorhodopsin Thin Films

(J. Glückstad, L.R. Lindvold, P.S. Ramanujam, and J. Juul Rasmussen)

Bacteriorhodopsin (bR), the light sensitive protein in the purple membrane halobacterium halobium, has been found to possess remarkable properties for optical storage and processing. Bacteriorhodopsin is a highly nonlinear optical material that has an extremely large third-order nonlinearity. A nonlinear Kerr coefficient of 10^{-4} cm^2/W has been reported. New mutants of bR have been reported to have 2 orders of a magnitude larger nonlinearities. We[1] recently reported the observation of dark spatial solitons in thin films of bR due to the nonlinearity of the material. Although the causes of this defocusing nonlinearity were not clear (thermal or optical), dark soliton-like structures were observed to evolve from a dark "hole" on a bright Gaussian background. We have also observed that a contrast reversal of amplitude-modulated images can be obtained by means of intensity dependent

phase changes in bR thin films.

The experimental scheme is based on a conventional 4-f setup. The input to the system consists of a pair of cross-wires which is imaged onto the output plane of the 4-f setup. The bR thin film is located in the spatial Fourier domain of the system. With the bR thin film in place, the contrast of the image at the output plane has to be reversed. A simple physical explanation of the effect can be given as follows: the Fourier transformation of the narrow object has a high spatial frequency content. The remainder of the Gaussian profile gives rise to a narrow and intense Gaussian distribution around the DC in the Fourier plane. Since the refractive index of the material is intensity dependent, a Gaussian phase distribution is formed around the DC, which can reach values much larger than π. Reimaging now the entire distribution, a contrast reversal of the image without additional loss of energy can be obtained[2].

An array illuminator based on the above scheme has also been developed. The large Kerr coefficient is exploited to implement a simple, robust, and energy efficient array illuminator that converts a uniformly expanded laser beam into an array of bright spots. This can be useful for illuminating arrays of photonic switching devices such as smart pixels, bistable elements, and optical thresholding devices.

An analytic model has been derived[3,4] for the light transformations through the system:

$$|\mathcal{O}(x',y')|^2 = \frac{2P}{r_0^2}\left|\sum_{k=0}^{\infty}\frac{(i\theta_0)^k}{k!(1+2k)}\exp\left(-\frac{\pi r'^2}{r_0^2(1+2k)}\right)\left(1+\frac{\Delta x_c\Delta y_c}{\Delta x\Delta y}\left[\exp(i\Psi)-1\right]\right)\right.$$

$$\left.-\exp\left(-\frac{\pi r'^2}{r_0^2}\right)\left[\exp(i\Psi)-1\right]\left(\frac{\Delta x_c\Delta y_c}{\Delta x\Delta y}-\sum_{m,n}\mathrm{rect}\left(\frac{x'-m\Delta x}{\Delta x_c},\frac{y'-n\Delta y}{\Delta y_c}\right)\right)\right|^2,$$

where the zero-order phase parameter is given by:

$$\theta_0 = \frac{4\pi L}{\lambda^3 f^2}n_2 P r_0^2\left[1+2\frac{\Delta x_c\Delta y_c}{\Delta x\Delta y}\left(\frac{\Delta x_c\Delta y_c}{\Delta x\Delta y}-1\right)(1-\cos\Psi)\right].$$

Plotting the above expression reveals an efficient and robust array illumination that can reach intensity levels that are almost up to four times stronger than the input intensity level. Surprisingly, the spot array does not manifest any "oscillations" in intensity level for increasing input power levels over a certain region, thereby increasing the robustness of the scheme. The area ratio value $\Delta x_c\Delta y_c/\Delta x\Delta y$ should be chosen in the interval $\{0,\frac{1}{2}\}$ in order to obtain an efficient spot array illumination. Area ratio values in the interval $\{\frac{1}{2},1\}$ on the other hand instead provide a "mesh-grid" illumination that could be useful for generating so-called structured light illumination for applications in machine vision.

Preliminary experimental results have been obtained with an amplitude input mask[5] (Fig. 4. The analytic expression for the output intensity is in this case simply given by the above equation omitting all $\exp(i\Psi)$-terms). Obviously, this has a strong impact on the intensity levels that can be achieved at the output side of the array illuminator. Nevertheless, the experiments act as a proof of principle also indicating that the scheme can be used for implementing dynamic contrast reversal of amplitude input objects.

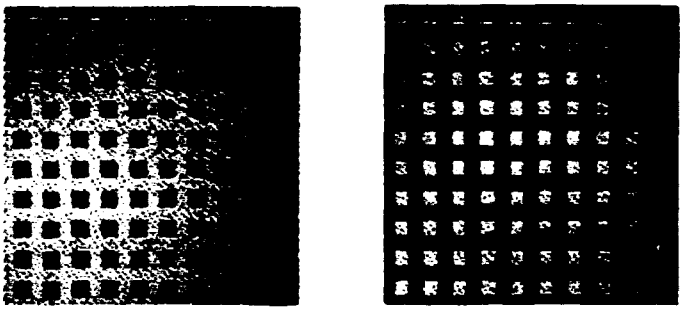

(a) (b)

Figure 4. (a) Image of input amplitude mask, spot size. (b) Image of contrast reversed input mask.

This work is supported by the ESPRIT programme (project no. 6863) and the Danish Natural Science Research Council.

1) Ramanujam, P.S., Lindvold, L.R. (1993). Appl. Opt. **32**, 6656-6658.
2) Ramanujam, P.S., Glückstad, J., Lindvold, L.R., and Rasmussen, J. Juul. (1994). Opt. Mem. and Neu. Net. **3**.
3) Glückstad, J. Ph.D. thesis (1994).
4) Glückstad, J. subm. Opt. Comm. (1994).
5) Glückstad, J., Ramanujam, P.S. (1994). Proc. IEEE/LEOS Boston, 318-319.

2.2.3 Chemically Enhanced Bacteriorhodopsin as a Real Time Holographic Recording Material

(L.R. Lindvold, H. Imam, and P.S. Ramanujam)

Holographic storage based on organic photochromic materials has been under investigation since 1970. One of the major problems of conventional organic photochromic materials has been unwanted side-reactions that have caused fatigue in the read-erase cycles. A material not suffering from this deficiency is bacteriorhodopsin, a naturally occurring photochromic protein, that partly constitutes the cell membrane in certain halophilic bacteria. The photochromic cycle (read-erase cycles of 1 million times have been reported) of the purple membrane is quite unique; the ground state has a broad absorption band with a peak centred at 570 nm (light adapted bacteriorhodopsin) and a metastable state centred at 412 nm with a thermal relaxation time of 10 ms. The metastable state offers two potential advantages. First, it can be stimulated either by electrical fields or photons to decay into the ground state in 200 ns. Secondly, the thermal relaxation time of this state can be extended by 5 orders of a magnitude by suitable chemical treatment of the purple membrane, without compromising the stimulated decay of 200 ns. This extension of the lifetime enhances the diffraction efficiency as well as the actinic sensitivity of bacteriorhodopsin when it is used as real time holographic recording material. A new method has been developed for this purpose using a crown ether (18-crown-6) to extend the lifetime by 3 orders of a magnitude[1].

The crown ethers are a family of cyclic, but saturated, ether compounds synthesised for the first time only 20 years ago. These compounds all share the name crown ethers due to their shape bearing resemblance to a regent's crown. One feature of great interest is its strong complexing properties towards cations like H^+, Li^+, Na^+, and K^+. As H^+ ions are involved in the photochemical process, the photocycle of bacteriorhodopsin can be modulated by the introduction of crown ethers. The presence of crown ether in a gelatin matrix would inhibit the capabil-

ity of the purple membrane to protonate the M-state, and subsequently decay to the ground state. The effect of doping a gelatin film containing bacteriorhodopsin is shown in Fig. 5.

This work is supported by the ESPRIT programme (project no. 6863).

1) Lindvold, L.R., Imam, H., and Ramanujam, P.S. (1994). "The Sensitometric Properties of Chemically Modified Bacteriorhodopsin Films", SPIE Proceedings **2429**, 22-33.

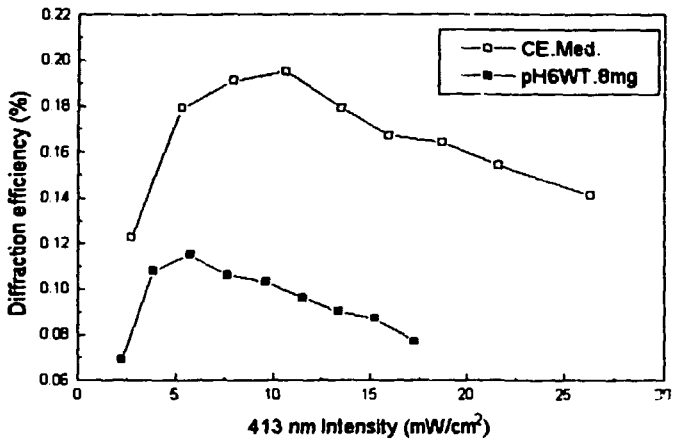

Figure 5. Relationship of diffraction efficiency of 633 nm probe with 413 nm write power for crown ether modified and unmodified vR_{WT} films. The weight ratio of bacteriorhodopsin to crown ether was 1:6.

2.2.4 An Optically Addressed Spatial Light Modulator Using Bacteriorhodopsin Thin Film as an Active Media

(H. Imam, L.R. Lindvold, and P.S. Ramanujam)

One of the key components in coherent optical image processing is a device known as a spatial light modulator (SLM). This device is capable of performing an incoherent to coherent conversion of light. A system capable of performing this task has been developed in the Optics and Fluid Dynamics Department during the course of this year[1]. The device is based on the photochromic protein, bacteriorhodopsin, immobilised in a polymer thin film (80 μm). It is, however, not this effect, but the photoinduced anisotropy[2] that is exploited in this device. This effect allows polarised incoherent light to control the polarisation of a laser beam via the photoinduced anisotropy in a bacteriorhodopsin thin film, which is faster than the photochromic process. In the experimental setup shown in Fig. 6 incoherent light from a halogen lamp is filtered through a Schott filter to take advantange of the broad action spectrum of bR, typically 570 nm ± 50 nm. To test the resolution of the device a USAF test target (chrome on glass) was imaged onto the SLM. The incoherent image formed was then read out by coherent light from a krypton laser @ 413 nm as this wavelength matches the maximum of the excited state in bR. The resolution obtained was 114 lines/mm, but this was due to a limitation of the optics in the system, not the material itself which has a resolution of at least 5000 lines/mm[2].

This work is supported by the ESPRIT programme (project no. 6863).

1) Imam, H., Lindvold, L.R., and Ramanujam, P.S. (1994). "A Photoanisotropic

Incoherent-to-coherent Converter Utilising a Bacteriorhodopsin Thin Film", accepted for publication in Optics Letters 1994.
2) Lindvold, L.R., Imam, H., and Ramanujam, P.S. (1994). "Spatial Frequency Response and Transient Anisotropy in Bacteriorhodopsin Thin Films", accepted for publication in Optical Review 1994.

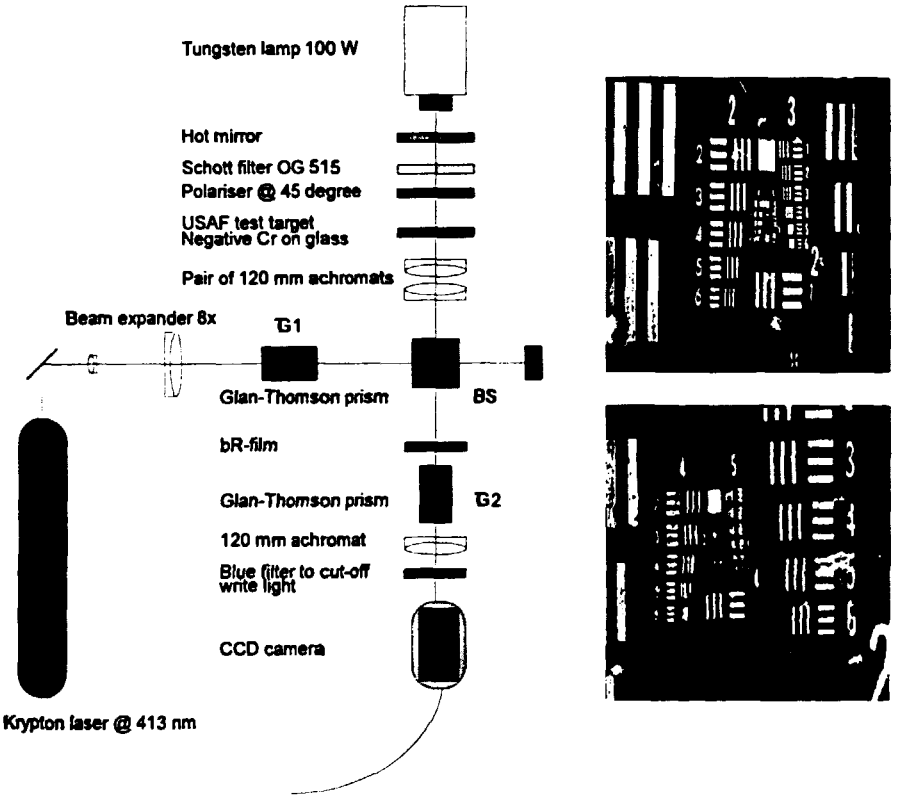

(a) (b)

Figure 6. (a) Optical setup for incoherent-to-coherent image conversion using bacteriorhodopsin thin film.(b) Images of the USAF test target showing the high resolution of the system.

2.2.5 Nonlinear Interactions between Gratings in Photorefractive Materials

(P.M. Petersen and P.E. Andersen (The Technical University of Denmark, Lyngby, Denmark))

Photorefractive materials are used in many applications such as neural networks, information storage, clock distribution, and optical computing. In these applications an important topic is the issue of crosstalk. We have recently investigated crosstalk in a $Bi_{12}SiO_{20}$ (BSO) optical interconnect[1]. In this device significant crosstalk is observed due to a nonlinear interaction between gratings. The nonlinear interaction between gratings is a consequence of the nonlocal response of the space charge field in the photorefractive medium and it can be analysed from a nonlinear solution to the band transport model. Our work has been concen-

trated on an angular multiplexed scheme for storage of optical information. The setup is shown in Fig. 7. The gratings are induced by the interference between

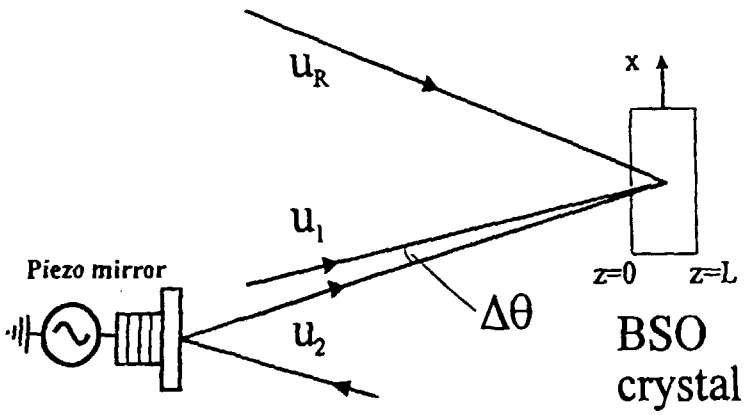

Figure 7. Setup for investigating nonlinear cross-talk between gratings in photorefractive materials.

one reference beam, U_R, and two object beams, U_1 and U_2, with a small angular separation. This creates two gratings, G1 and G2, caused by the interference of the reference wave with each of the two object waves and a third grating, G3, caused by the interference between the two object waves. This third grating is usually neglected due to the small separation angle between the object beams. We show, however, that even though G3 itself is negligible, it introduces nonlinear combinations of gratings which in turn lead to significant crosstalk between the fundamental gratings G1 and G2. We probe the nonlinear mixing of gratings using a phase shifted object beam. By applying a proper phase shift in the object beam U_2 we can selectively switch off grating G2 without affecting the total intensity in the BSO crystal. The crosstalk between the gratings can be estimated from the diffraction efficiency in G1 before and after G2 has been switched off. Using this method we have experimentally obtained crosstalk larger than 50%. Furthermore, we have investigated theoretically the nonlinear mixing of gratings by using the band transport model. Due to the nonlinear nature of this model the space charge-field contains spatial frequencies that are mixings of the fundamental gratings G1, G2, and G3. Using a nonlinear solution to the band transport model we have shown[2)] that nonlinear mixing of gratings may cause a change in the diffraction efficiency up to 50% compared with a usual linear solution to the model. The unexpected strong nonlinear interaction has important consequences for many photorefractive applications with multiple beam interactions, as for example in photorefractive optical interconnects and photorefractive storage.

1) Andersen, P.E., Petersen, P.M., and Buchhave, P. (1994). "Crosstalk in Dynamic Optical Interconnects in Photorefractive Crystals", Appl. Phys. Lett. **65** (3), 271-273.

2) Andersen, P.E., Petersen, P.M., and Buchhave, P. (1994). "Crosstalk in Photorefractive Optical Interconnects Due to Nonlinear Mixing of Gratings", Optics and Photonics News/December 1994, 12-13.

2.2.6 Photorefractive Interference Filters

(C. Dam-Hansen, P.M. Johansen, P.M. Petersen, and B. Hurup Hansen)

The application of photorefractive materials for ultra-narrow bandwidth optical filters has gained a growing interest during the last few years. The high reflectance and high wavelength selectivity of volume reflection phase gratings are being used to produce filters with subangstrom bandwidth. Photorefractive crystals of iron-doped lithium niobate have been chosen as the recording material because of the possibility of long-time storage. The work done here has been based on filters with centre wavelengths in the visible spectrum at 514.5 and 413 nm. The filters are induced in a reflection geometry setup, with two counterpropagating expanded laser beams. The inherent nonlocal response of photorefractive materials causes intensity and phase coupling of the writing beams. The intensity coupling as well as the absorption cause the modulation of writing beams to vary through the crystal. This local modulation index can be controlled by varying the intensity ratio of the incident beams. The amplitude of the recorded refractive index modulation, in the small modulation approximation, is linearly proportional to the intensity modulation. Because of this, the filter response will depend on the direction of propagation of the probe beam. This is illustrated in Fig. 8 where the spectral response of a filter has been measured for a probe beam propagating in the positive and negative directions of the z-axis. This spectral response has been deduced from combined angular and temperature measurements. The filter has been written in a 15 mm long iron-doped lithium niobate crystal, with a measured absoption coefficient of $1.03\ cm^{-1}$. The absorption limits the obtainable maximum reflectance, which is approx. 31% for probing in the positive z-direction. The reflectance is much lower, approx. 11%, for probing in the opposite direction. The solid lines are the calculated spectral response, assuming a local modulation index as shown in the inset. The inset also shows the variation of the writing beam intensities. The theory gives a good description of the maximum reflectance and the width of the response curves, but it does not explain the enhanced sidelobes and large asymmetry. This asymmetry indicates a nonuniformity in the spatial frequency of the filter grating, which has not yet been explained.

The centre wavelength of the filter is 514.5 nm. The wavelength bandwidth given by the full width half max. value is determined from Fig. 8 to be 0.1 Å (positive z-direction). The temperature sensitivity of the centre wavelength has been measured to be (0.047 ± 0.003) Å/K. The narrow thermal response means that the crystal has to be temperature stabilised. By controlling the temperature of the crystal to within 0.1 K an absolute wavelength control of 0.005 Å is possible. For this purpose custom designed ovens for the different lithium niobate crystals have been produced in the department. The temperature controller unit employs a temperature sensor and a feedback loop controlling the power to a Peltier element. The oven allows for the illumination of two opposite faces of the crystal. The estimated accuracy of the crystal temperature is approx. 0.05 K, and the dynamic range is 15-35°C. The filters are thereby tunable within a range of 0.9 Å, which is ten times the bandwidth.

This work is supported by The Danish Technical Research Council under grant no. 16-5220-1.

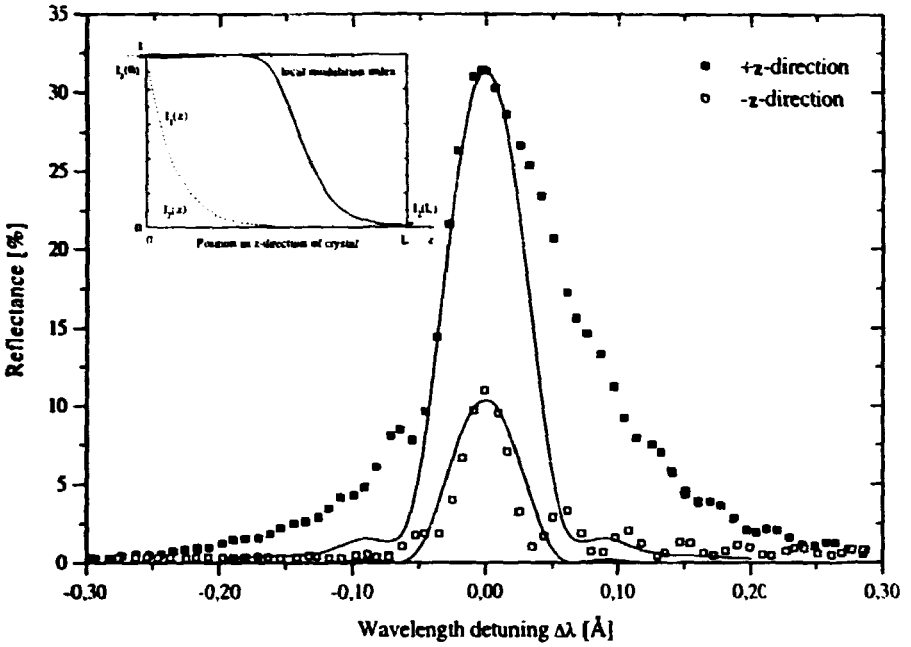

Figure 8. Measured filter reflectance as a function of the wavelength detuning for the two propagation directions of the probe beam. The normalised intensities of the writing beams and the resulting local modulation index are shown as a function of the position in the inset. The incident intensity ratio is $I_1(0)/I_2(L) = 48$.

2.2.7 New Subharmonic Gratings in Photorefractive Media

(H.C. Pedersen and P.M. Johansen)

When two mutually coherent laser beams interact inside a photorefractive crystal, an interference pattern is generated. By shifting the frequency of one of the beams with respect to the other, the interference pattern starts moving. If a photorefractive medium is exposed to such a moving interference pattern, which may be called a wave of light intensity, a corresponding wave of refractive index (running grating) is generated in the medium. In the linear case this wave of refractive index has the same temporal and spatial frequency as the intensity wave. In the nonlinear case, however, it is possible for so-called subharmonic waves to arise, where the spatial frequencies are 1/2, 1/3, or 1/4 of that of the fundamental frequency. In the photorefractive group the so-called K/2 subharmonic generation appearing at half the fundamental frequency is investigated.

In all subharmonic experiments presented till now, the subharmonic grating vectors were parallel to the fundamental grating vector. However, at Risø new subharmonic gratings have been observed[1)], where the grating vectors are no longer parallel to the fundamental grating. This effect can be observed by reading out the generated gratings with an auxiliary laser beam. This is shown in Fig. 9. As can be seen, the first-order spots and the zeroth-order spot are aligned. In conventional subharmonic experiments the subharmonic spots would also have been aligned along the same line. However, as is seen in Fig. 9, this is certainly not the case in the present experiment. In the photorefractive group we believe that these new experimental results will lead to a more complete understanding of the dynamic process in photorefractive crystals.

This work is supported by The Danish Natural Science Research Council under grant no. 11-0921-1.

1) Pedersen, H.C. and Johansen, P.M. (1994). "Observation of Angularly Tilted

Subharmonic Gratings in Photorefractive Bismuth Silicon Oxide", Opt. Lett. **19**, 1418.

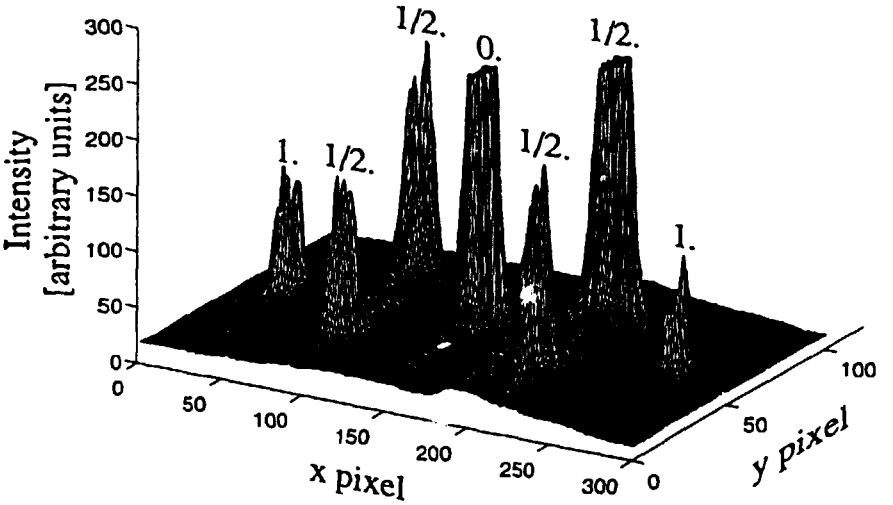

Figure 9. Diffraction pattern when reading out the new subharmonic gratings. The peaks marked with "1" correspond to diffraction in the fundamental grating (first order), "0" corresponds to the directly transmitted read-out beam (zeroth-order), and "1/2" corresponds to diffraction in the new subharmonic gratings.

2.2.8 Wave Coupling in Photorefractive Cubic Media far from the Paraxial Limit

(H.C. Pedersen and P.M. Johansen)

Two-wave mixing in photorefractive media has been studied extensively during the last 15 years. The physical process is as follows: two mutually coherent laser beams are incident to a photorefractive crystal, where they form an interference pattern. Due to the photorefractive effect a corresponding refractive index pattern arises as a refractive index grating. The laser beams diffract in this grating and exchange energy. In other words: the two laser beams are affected in intensity and polarisation by the grating they have induced themselves. This process is referred to as self-diffraction.

In the theoretical models used up till now, a so-called paraxial approximation is applied in which it is assumed that the angle between the two interfering beams is small. In the photorefractive group at Risø we have succeeded in developing a two-wave mixing model which also accounts for large angles between the beams[1]. The large angle effects (or aparaxial effects) are analysed in cubic crystals, where significant changes between the paraxial model and the exact model have been discovered. An example of this is shown in Fig. 10, where the coupling efficiency versus fringe spacing of the induced grating has been plotted. It is seen that a deviation of more than 10% between the two models can be obtained when the fringe spacing gets below 0.5 μm. This work si supported by The Danish Natural Research Council under grant no. 11-0921-1.

1) Pedersen, H.C. and Johansen, P.M. "Analysis of Wave Coupling in Photorefracitve Cubic Media far from the Paraxial Limit", to be published in J. Opt. Soc. Am. B, **12** (4), April 1995.

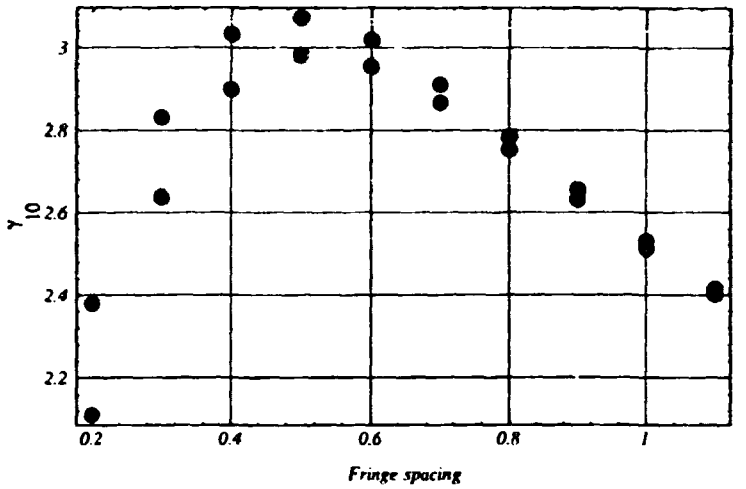

Figure 10. Coupling efficiency (z = 10 mm) between two incident beams in a 10 mm (interaction length) $Bi_{12}SiO_{20}$ crystal versus fringe spacing (in μm) of the induced grating. Grey spots: paraxial model; black spots: exact model.

2.3 Diagnostics

2.3.1 Ocean Optics

(S.G. Hanson, V. Zavorotny*, J. Churnside*, and J. Wilson* (*Environmental Technology Laboratory, NOAA, Boulder, CO, USA))

The interaction of electromagnetic waves especially in the visible spectrum has been investigated in order to benefit from existing imagery obtained in the microwave spectrum[1)] or with the aim to introduce new concepts for surface wave measurements.

Microwave imagery from conventional airborne side looking radars reveals surface structures. The modulation depth of these structures is highly dependent on the polarisation of the transmitter and receiver to a degree which cannot be explained by the single scattering Bragg theory. Multiple scattering inside the troughs of gravity waves has been theoretically analysed in order to quantify this contribution to the backscattering cross section. It has been shown that monostatic backscattering cross section for horizontally polarised radiation at large angles of incidence can be increased by 3 dB (see Fig. 11). This gain is primarily due to enhanced backscattering arising from the high reflection coefficient for horizontally polarised radiation as compared with vertically polarised radiation in connection with the monostatic setup[2)]. For grazing angles this effect may provide a tool for gathering information on minor changes in scales of larger structures, i.e. gravity waves.

The use of lasers to probe velocities of particles or solid surfaces has been used extensively in the past, the basic principle being the formation of a fringe pattern in the measuring volume. Scattering structures passing the volume will emit a field which will give rise to a frequency modulated signal current giving the velocity. An alternative setup well-suited for long-range measurements has been proposed, based on having a fringe pattern perpendicular to the optical axis by emitting two longitudinal modes from the laser. This fringe pattern moving at the velocity of light is projected onto the ocean surface and only structures matching the fringe spacing will effectively contribute to the temporal modulation of the backscattering signal. This allows for measurement of the gravity wave spectrum and the associated phase velocities and, thus, the surface current by variation of

the mode separation in the laser. A theoretical analysis and a discussion on the influence of various secondary parameters have been offered.

Incoherent light backscattered from the ocean primarily arises due to scattering from suspended particles. This implies that the received light has suffered two penetrations of the interface between the water and ambient air providing a received signal which depends on the angle of incidence, the polarisation of the light, and the amount of suspended scatterers. If two images are recorded with horizontally polarised and vertically polarised light, the ratio of the intensities will be given only by the angle of incidence and the refractive index of the water. If two images with two orthogonal polarisations are recorded, the ratio between the pixel values can be calculated and the distribution of angles of incidence over the entire frame can be found[3]. This enables temporal tracking of the wave pattern during an extended period, thus providing information on the wave spectrum and spatial correlations of breakers and capillary waves with respect to the large-scale gravity waves.

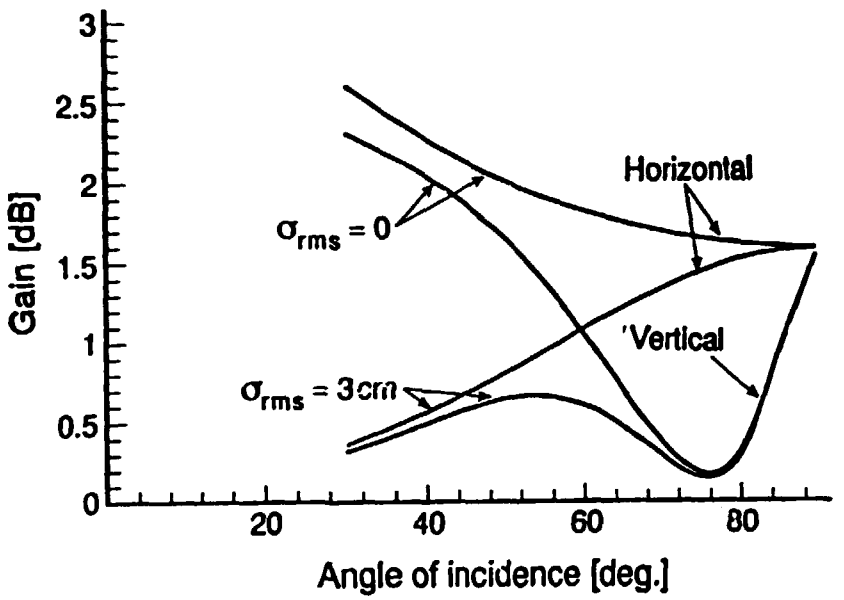

Figure 11. Increase in backscattering cross section at resonance for horizontal and vertical polarisation. The result is shown for a microwave wavelength of 3 cm (X-band) and for a small-scale surface roughness of 3 cm and 0 cm.

1) Hanson, S.G. and Zavorotny, V.U. (1994). "Polarization Dependency of Enhanced Multipath Radar Backscattering from an Ocean Surface", submitted to Waves in Random Media, December 1994.

2) Churnside, J. and Hanson, S.G. (1994). "Effect of Penetration Depth and Swell-generated Tilt on Delta-k Lidar Performance", Applied Optics, **33**, No. 22, April 1994.

3) Churnside, J., Hanson, S.G., and Wilson, J.J. (1994). "Determination of Ocean Wave Spectra from Images of Backscattered Incoherent Light", to be published in Applied Optics, January 1995.

2.3.2 Measurement of Rotational and Linear Velocities

(S.G. Hanson, L. Lading, and B H. Hansen)

The industrial applications of optical technologies have prospered from the widespread use of electronic and optical subsystems in consumer products. The lowering of the prices of laser diodes, video-chips, and powerful processing electronics has opened for a wider range of feasible implementations. When this is combined with the possibility of implementing complex optical transformations in one holographic optical element, the possibility of new, low-cost optical sensors has been attained.

We have implemented a series of optically based systems for measurement and monitoring of mechanical translations. This includes measurement of linear velocity, either by the time-of-flight method or by the Doppler method. Rotational speed and torsional vibrations can likewise be measured by a Doppler scheme or by a speckle correlation method. Two compact systems based on speckle correlation systems have been implemented. Fig. 12 shows the entire time-of-flight anemometer including optics and electronic processor mounted in the same casing[1]. The optical components have been reduced to one laser diode, two detectors, a mirror, and one complex holographic optical element. The latter provides the necessary beam shaping for the transmitter as well as the focusing and redirection of the reflected light from the target toward the detectors. Alignment is inherent in the holographic element due to the simultaneous recording of transmitter and receiver. Consequently, a change of wavelength or minor displacements of the holographic element will have the same impact on the transmitter and the receiver, leaving the overall performance unchanged.

Minor changes in the time-of-flight system for measuring linear velocities are necessary in order to convert the setup into a torsional vibrometer[2]. The instantaneous rotational velocity is here given by the estimate of the position of the maximum crosscorrelation between the two detected signals. The detectors in this configuration are placed in the Fourier plane with respect to the target. The detected signals are therefore related to positions on the target having a slope causing light to be reflected toward the detector. Therefore, the measured time delay will depict the angular velocity without respect to the radius of curvature of the shaft and its distance from the system.

Whole field monitoring of displacements for a solid body between two states has been achieved. A robust differential electronic speckle interferometry (ESPI) system has been built based on a holographic optical element as shearing element. The robustness of the system is achieved by replacing the ordinary ESPI concept with a "common path interferometer" concept. Both interfering beams originate from the target, thus eliminating the need for a local reference beam in the system. A disturbance of the beam during the passage toward and back from the target is balanced out in this setup. Wavelength independency and reduced sensitivity to lack of temporal coherence of the laser are facilitated by the use of a holographic optical element.

1) Hanson, S.G. and Lindvold, L.R. (1994). "High Accuracy Sensor for Dynamic Measurements Based on Holographic Optical Elements, Semiconductor Lasers and Detectors". Technical Digest: 1994 Conference on Lasers and Electro-Optics Europe, IEEE September 1994, CTuD1.

2) Hanson, S.G. and Hansen, B.H. (1994). "Laser-based Measurement Scheme for Rotational Measurement of Specularly Reflective Targets", SPIE **2292**, Fiber Optic and Laser Sensors XII, 1994, 143-153.

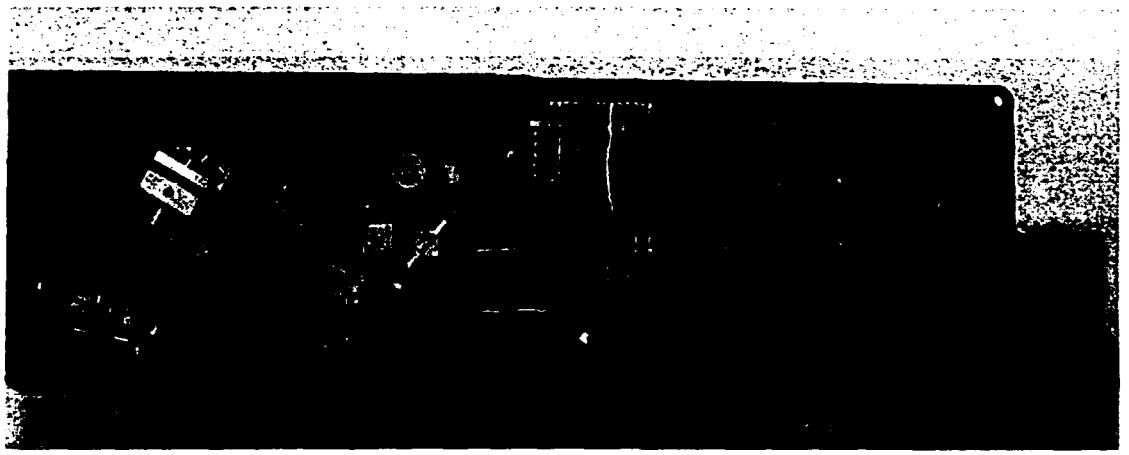

Figure 12. Compact laser time-of-flight velocimeter based on a holographic optical element.

2.3.3 Integrated Optoelectronic Sensors

(L. Lading, S. Hanson, and L.R. Lindvold)

For a number of years the department has worked with different measuring systems mostly based on quasi-elastic light scattering. Most of the systems considered are for the measurement of the dynamics of fluids and solid objects. Systems for this type of measurement are generally rather complex and require delicate alignment because they are based on optical interference or mixing.

It has been demonstrated that the use of holographic optical elements can provide for a drastic simplification of the mechanical layout of such systems. The reason for this is that many optical elements can be multiplexed into a single or few elements. The calibration of measuring systems based on quasi-elastic light scattering depends on the optical wavelength and a geometrical factor. Using holographic optical elements (diffractive elements), it is possible to make systems where the calibration is independent of the wavelength: changing the wavelength causes a change of the geometrical factor that exactly compensates for the effect of the wavelength change on the calibration. This fact makes it possible to utilise low-cost unstabilised semiconductor lasers instead of gas lasers.

The mechanical complexity can be further reduced by combining waveguiding and diffractive structures on a single substrate. Doing this essentially eliminates the space required for free space propagation (that is otherwise essential). The concepts are illustrated in Fig. 13. Figure 13(a) shows a conventional system for velocity measurements by the time-of-flight method. It is based on conventional refractive optics and birefringent elements. Figure 13(b) shows an implementation with a holographic optical element. Both receiver and transmitter are incorporated in the element. By partly multiplexing - which is impossible with simple refractive elements - the calibration is made independent of the wavelength. It is exclusively given by the diffractive structure in the holographic element. Figure 13(c) shows a conceptual layout for a fully integrated version. The main difference relative to Fig. 13(b) is that the free space propagation between laser/detectors and holographic element is replaced by 2D guiding surface structures. The technology of the latter configuration is the subject of a newly initiated project.

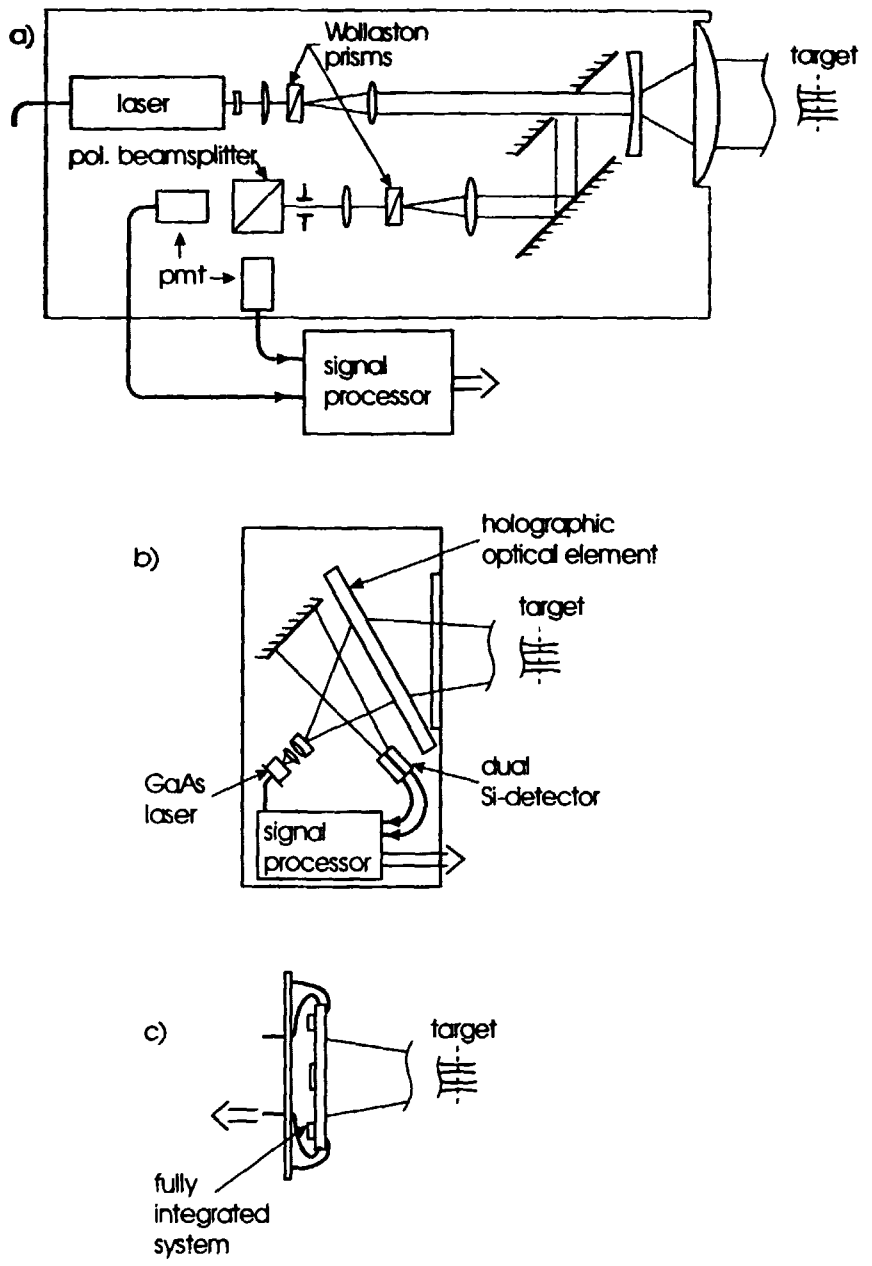

Figure 13. Laser velocimeter implemented with (a) conventional refractive optics, (b) holographic optical element, and (c) integrated optics.

2.4 Information Processing

2.4.1 Neural Networks for Image Processing

(S. Sloth Christensen and T. Martini Jørgensen)

In recent years image processing has become important as the demand for nondestructive quality control has increased. It is, however, a nontrivial task to extract the required information from the high-dimensional image data space. The introduction of a vision system on a production line does thus often require the development of an algorithm designed specifically for one product. It is therefore desirable to develop tools that will facilitate the adaptation of image processing systems to different tasks. Our research has focused on this problem and we have

tried to come up with a flexible and easily adaptable image processing scheme.

There are two main steps in image processing:

- Preprocessing of the image data
- Classification of the preprocessed image data

The classification of preprocessed data can be performed in a number of different ways. We have investigated the use of artificial neural network, ANN, methodologies for classification purposes. The advantage of ANNs is that a classification system can be built based on a set of training data. The development process of the classifier is thus reduced to the task of collecting a representative set of image data. The same basic classification system may consequently be applied to different image processing tasks without any changes to the code.

In order to obtain reliable classifications there is, however, a need for preprocessing of the image data. It can, though, be difficult to know which preprocessors are beneficial for a specific task. To overcome this problem we use an information measure developed for the WIZARD type of ANN. Based on this information measure, we have devised an algorithm that from a set of filters allows us to select the filters that provide the information required to perform the desired classification task.

The information measure is based upon the Shannon entropy and the "leave n-out"-crossvalidation concept. The basic idea is to learn as much as possible while at the same time minimising the storage requirements. Such a strategy improves the generalisation strategy of the system.

These basic tools allow us to automate the evaluation of different preprocessing methods and to use a general classification system. This does simplify the construction of vision systems[1)]. It is, however, still necessary to devise an appropriate illumination for each vision task. The performance of such a system is still highly dependent upon the set of preprocessors available and the performance of the ANN.

A major part of the work mentioned above has been carried out as part of an EUREKA project. The partners are: Rambøll Hanneman & Højlund (DK), Applied Bio Cybernetics (DK), and BICC (GB).

Other ANN activities

A Brite-Euram project for the handling of flexible materials has been completed successfully. We have developed an ANN-based image processing system that on the basis of 2D and 3D visual information generated control information for a robot controller[2)]. The other partners in the project were: The Danish Meat Research Institute (DK), University of Bristol (UK), Ricardo Hitec (UK), and Siemens (D).

An ESPRIT project has been started, where the task is to analyse complex 3D image data. The other partners in this project are: Siemens (D), Robotica (E), and 3D Scanners (GB).

1) Jørgensen, T.M., Christensen, S.S., Andersen, A.W., Liisberg, C. (1994). "Optimization and Application of a RAM Based Neural Network for Fast Image Processing Tasks". In: Intelligent Robots and Computer Vision 8: Algorithms and Computer Vision. Conference on Intelligent Robots and Computer Vision 8: Algorithms and Computer Vision, Boston, MA (US), 31 Oct. - 2 Nov. 1994. Casasent, D.P. (ed.), (The International Society for Optical Engineering, Bellingham, WA, 1994) (SPIE Proceedings, 2353) 328-338.

2) Andersen, A.W., Christensen, S.S., Jørgensen, T.M. (1994). "An Active Vision System for Robot Guidance Using a Low Cost Neural Network Board". In: Proceedings EURISCON '94'. Vol. 1: Stream A. European Robotics and Intelligent Systems Conference, Malaga (ES), 22-25 Aug. 1994. (AMARC. University of Bristol, Bristol, 1994) 480-488.

2.4.2 FFT Processor

(A. Skov Jensen, E. Rasmussen, J. Bundgaard*, and K.M. Enevoldsen* (*Engineering and Computer Department, Risø))

A fast Fourier transform (FFT) card for a PC with an EISA bus has been designed and constructed in a cooperation between the Optics Section and the Engineering and Computer Department. The FFT processor has been tested for simulations of 2D optical applications. The advantage of using a hardwired FFT processor as compared with an optical FFT processor is flexibility: testing an optical Van der Lugt correlator or a joint transform correlator, e.g., demands a vast amount of work in connection with the production of filters and with the optical stability of the transforming lenses.

When comparing the FFT card with ordinary computer programming, the advantage is first of all speed. If a simulation requires testing of complicated processing facilities additional to the FFT and speed is not a major problem, the hardwired FFT should be avoided due to the relatively complicated assembler programming of the FFT card.

The complex Fourier transform of an image of 1024×1024 points (16 bits) takes 1.65 seconds to perform. This includes the time transferring the data from the PC memory to the FFT card and back. The actual time for FFT in itself is only .37 seconds which means that the overhead is approx. 50% for transport and rearrangement of data. The time required for a matched filter correlator is 3.36 seconds and 3.65 seconds for a joint transform correlator for a 1024×1024 data arrangement. Due to the overhead, the speed is close to being proportional to the data length.

Examples of an FFT of a square and its log-polar transform are shown in Figs. 14a and b.

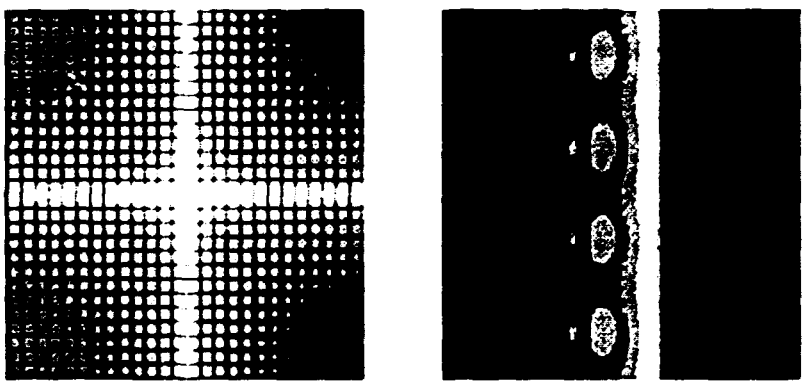

(a) (b)

Figure 14. (a) shows the FFT of a square, whereas (b) shows the log-polar transform of the FFT of a square.

2.4.3 Computer-generated Lens Array for Local Correlation

(A. Skov Jensen, E. Rasmussen, and E. Eilertsen)

Lens arrays or fly eyes are very appealing from an optical point of view, but the question is what they can be used for. The localised structure of the lenses in the array means that information can be processed in parallel in separated channels. Optical networks for communication are an example of this. Another potential

application is the processing of local area in an image, for instance doing local correlation. This can be used for processing of optical flows, i.e. decoding of the velocity profile of a moving scene (PIV - particle image velocimetry) and stereoimage decoding. Correlation of images can be done optically with a joint Fourier transformer, where the Fourier transforms of the two images to be correlated are superimposed on a squaring device (a light-to-light spatial light modulator) followed by another Fourier transform. This is a well known technique for global images. With two lens arrays and a spatial light modulator (bacteriorhodopsin) a very compact local correlator can be constructed.

Lens arrays can be produced with refractive or diffractive lens elements. In many cases the refractive lenses are to be preferred, but in the case of a compact local correlator it is advantageous to use diffractive lenses. A sketch of a possible local correlator is shown in Fig. 15(a).

To separate the diffracted light from a single lens from all the undiffracted light from all the other lenses, a diffraction angle close to 90 degrees must be used (see Fig. 15(a)). In Fig. 15(b) a test sample of a diffractive lens array is shown.

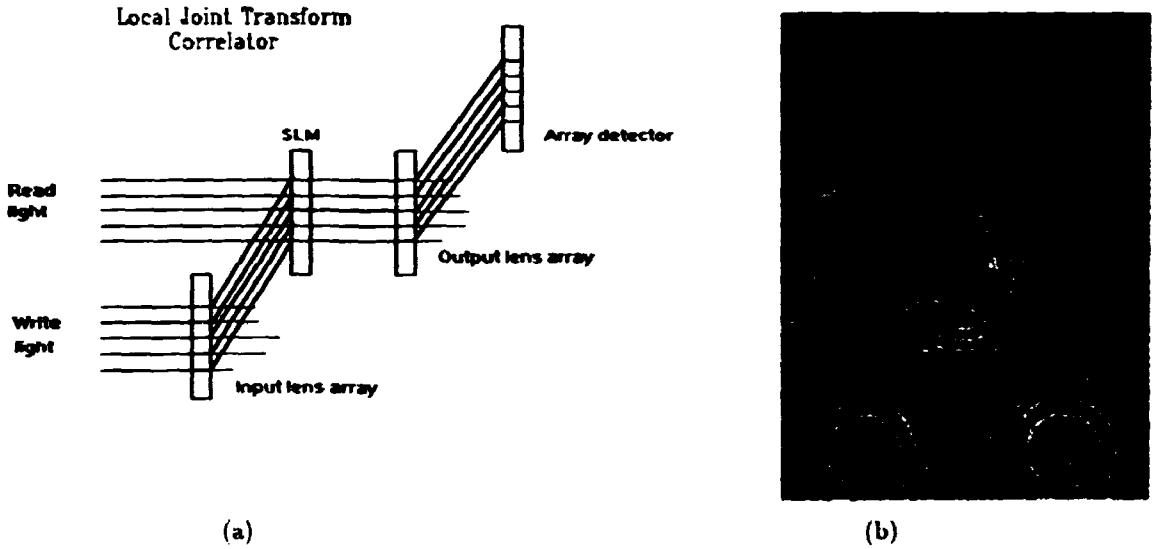

Figure 15. (a) A local joint transform correlation. (b) lens array with overlapping lenses.

3 Continuum Physics

3.1 Introduction

Nonlinear dynamic processes as 'self-organisation', 'localisation', and 'collapse' are fundamental phenomena which are showing up in an increasing number of different physical systems. Despite the apparent differences in the media in which the phenomena are observed, the generic properties of the nonlinear processes are very similar. Thus, strong vortical structures with similar properties are found in the atmospheres and oceans of rotating planets and in the hot plasma inside big fusion experiments as, e.g., tokamaks and stellarators. Also, the spontaneous formation of regular structures and patterns has many common features in rotating fluids, magnetised plasmas, and nonlinear optical media.

The investigations of the fundamental properties of the nonlinear dynamic processes are performed by theoretical, numerical and experimental studies, and these three angles of approach supplement and stimulate each other. In this way, theoretical predictions are tested by detailed numerical studies, numerical results are verified by experimental studies, and experimental studies give impulses to new theoretical and numerical investigations.

In addition to these fundamental studies, the theoretical and numerical models are also applied to more practical problems in which extra, complicating effects - such as solid boundaries in ordinary fluid flow, or more complex interactions in a magnetised plasma - are taken into account. Another application of the research is the development of a new laser diagnostic for measurement of plasma turbulence in a large European plasma device. This diagnostic will allow for measurements of dynamic processes that are of direct relevance to the theoretical and numerical studies.

Numerical codes are improved

The traditional methods applied in computational fluid dynamics are not adequate for the detailed investigations necessary in our studies. We have already developed several new codes based on 'spectral methods' that have superior accuracy properties as compared with the traditional methods. These 'first generation' spectral codes are being used in our studies of fundamental nonlinear phenomena, but they are limited to simple geometries such as an infinite periodic array, a periodic channel, or an annulus. In order to be useful for numerical studies of flows of more practical relevance, the algorithms need major development. This process involves employing new ideas from applied mathematics and numerical analysis. In 1994, several major steps were taken in this direction in close collaboration with research groups working with applied mathematics at American universities. These steps include the development of a multidomain, spectral algorithm employing a new method of imposing boundary conditions for compressible flows, a new algorithm for pressure calculation in incompressible flows, and a new method for accurate computation of incompressible flows in double bounded domains. All these schemes have in common that they have enhanced the accuracy of the computations significantly with very little, if any, extra cost of computer time. These methods need further development for computations of flows in three-dimensional regions with complex geometries.

Particles not easy to track

Even in an apparently very simple flow field, the trajectories of particles released in the flow can become extremely complicated or chaotic. In order to track individual particles with high accuracy in our numerical simulations of both simple and complex flow fields, a special particle tracking algorithm has been implemented. Based on this algorithm, new results concerning particle motion near simple vortical structures under the influence of viscous damping have been obtained. The high precision of these calculations also forms the basis of a new collaboration with Danish industry, where the company Dantec Measurement Technology is interested in the numerical results as a reference for their whole field, particle image velocimetry (PIV) diagnostic system for fluid flow. Based on the initial results, a long series of numerical comparisons is planned.

In parallel to the numerical simulations, particle tracking is also performed in laboratory experiments. Here, the motions of a large number of particles suspended in the flow are recorded on videotape. The individual frames on this tape are subsequently analysed by a computer program. In another joint project with Dantec Measurement Technology, Risø's particle tracking results are compared with the results obtained by Dantec's PIV system.

Leaps between dimensions

The dynamic behaviour of two- and three-dimensional systems is fundamentally different. Thus, one cannot simply apply the results obtained from two-dimensional studies on three-dimensional problems, and vice versa. Particularly interesting phenomena occur when the flow spontaneously changes from one dimensionality to another. Two different series of laboratory experiments have been conducted to study such transitions. In one case, a three-dimensional vortex ring was injected into a horizontally stratified fluid. Due to this stratification, the vortex ring collapses into a pancake shaped dipolar vortex with two-dimensional properties. In the other experiment, two parallel vortex columns were injected into a water tank with uniform density. Due to effects caused by interactions between the ends of the vortex columns and the walls of the tank, a three-dimensional disturbance was generated. This disturbance caused the two columns to connect at the ends and to contract lengthwise. As a result, a three-dimensional vortex ring was formed. This ring quickly accelerates to a much higher speed than the velocity of the initial vortex columns.

Structures form spontaneously

In 1994, a number of investigations of spontaneous structure formation in different physical systems have been performed. Numerical studies have shown details of self-organisation and structure formation in liquids and gases that are forced by differential rotation over a narrow region. Other numerical studies have proven the formation of organised dipolar vortices from turbulent initial conditions in two- dimensional flows. In the field of nonlinear optics, several theoretical and numerical investigations have been conducted in processes known as 'localisation' and 'collapse'. Localisation indicates a redistribution of the light intensity redistributed into a region of limited extent, and collapse describes a more dramatic, but idealised, process in which the optical field within a finite time interval contracts into a single point, where the intensity becomes infinitely high. Nonlinear optical experiments have also been performed. These experiments clearly demonstrated pattern formation in thin films of bacteriorhodopsin.

New laser diagnostic for fusion research

Despite many years of intensive research and development towards the use of magnetically confined plasmas for the production of energy, much remains unknown about the basic physical processes inside the plasma. There is an ongoing need for the development of new diagnostic techniques that allow detailed measurements to be performed without disturbing the plasma. Within the framework of EURATOM, we are developing a time-of-flight type laser anemometer for measurements of electron density fluctuations in plasmas. This system is currently being tested at Risø using a turbulent air jet. Upon successful completion of these tests, it is planned to move the system to the Wendelstein VII-A stellarator in Garching, Germany, for measurements on a large-scale plasma device.

3.2 Development of Spectral Algorithms

3.2.1 Spectral Methods on Unstructured Grids

(J.S. Hesthaven, M. Carpenter (ICASE/NASA Langley Research Center, USA), and D. Gottlieb (Division of Applied Mathematics, Brown University, USA))

Traditionally, spectral methods require interpolation at the nodes of a gauss type quadrature formula. Thus, the mesh points are predetermined and inflexible. In

particular the distribution of grid points is denser in the neighbourhood of the boundaries which leads to considerable difficulties, even in one dimension, since for many problems the information is given in points different from those required by the spectral method. This fact manifests itself more severely when dealing with multidimensional problems and seems to limit the applicability of spectral methods to simple domains. In two dimensions one can easily apply spectral methods to rectangular domains but the extension to other domains is not trivial.

A novel approach to overcome this limitation is to construct spectral methods from first principle. The unknown function is approximated by a general Lagrange polynomial from which differentiation operators are also obtained.

The key idea in the unstructured spectral methods is that an equation does not have to be satisfied at the same points as the derivatives are evaluated. For example, the derivative can be carried out by Lagrange interpolation at any particular point whereas the equation is satisfied in a Galerkin-, tau-, or by collocation-sense at a different set of points - 'ghost points'.

In spectral methods on unstructured grids, the boundary conditions are applied through a penalty method. This allows us to prove asymptotic stability of the methods. The accuracy of the scheme is obtained by choosing the penalty function correctly, thus allowing for proof of equivalence with the well known Galerkin-, tau-, or collocation formulations of Legendre methods.

Hence, this scheme enables us to apply spectral methods in circumstances where the grid points are not nodes of some gauss quadrature formula. Although the theoretical framework allows for multidimensional approaches by employing flux splitting, spectral methods on unstructured grids have only been thoroughly tested for one-dimensional hyperbolic problems. We are presently working on developing this approach to allow for solving problems in triangular domains. A successful implementation of such a scheme will allow us to perform spectral calculations of problems in complex domains by triangulation, similar to the approach followed for traditional low-order finite-element methods, and with similar geometric flexibility.

3.2.2 A Stable Penalty Method for the Compressible Navier-Stokes Equations

(J.S. Hesthaven and D. Gottlieb (Division of Applied Mathematics, Brown University, USA))

When addressing wave-dominated, dissipative problems, one is often forced to introduce an artificial boundary for computational reasons, e.g. for simulating open boundaries and when applying a multidomain technique. This introduces the well known problem of specifying appropriate boundary conditions at the artificial boundary. For purely hyperbolic problems, it is well known that enforcing these boundary conditions through the characteristic variables leads to a stable approximation. However, for dissipative wave problems the procedure is considerably more complicated.

We have developed a unified approach for dealing with open boundaries and subdomain boundaries when performing simulations of the three-dimensional, compressible Navier-Stokes equation in conservation form. The scheme converges uniformly to the singular limit of vanishing viscosity and, hence, is also valid for the compressible Euler equation.

In the development of the scheme, we apply the energy method to the linearised, constant coefficient version of the continuous problem to obtain energy inequalities that bound the temporal growth of the solutions to the initial-boundary value problem. This approach allows us to derive a novel set of boundary conditions of the Robin type[1)] which ensure the complete problem to be well-posed. This

result is obtained for the Navier-Stokes equations given in general curvilinear coordinates.

It has traditionally been found difficult to apply boundary conditions of the Robin type when doing psendospectral simulations of nonlinear equations. We have shown how it is possible to implement the boundary conditions as a penalty term which allows for enforcing open boundary/patching conditions of a very general type. An attractive feature of the penalty method is that one may prove asymptotic stability of the semidiscrete scheme, thus gaining confidence in the computed results when addressing unsteady problems where long time integration is required.

A multidomain scheme, where the patching of subdomains is based on a penalty method, is strictly local in space, thus making it well suited for implementation on contemporary, parallel computer architectures with distributed memory[2].

The scheme has been successfully implemented to obtain multidomain solutions of one- and two-dimensional compressible, viscous flows with open boundaries. Examples include steady, transonic quasi-one-dimensional viscous nozzle flow (see Fig. 16) and unsteady flow around an infinitely long cylinder.

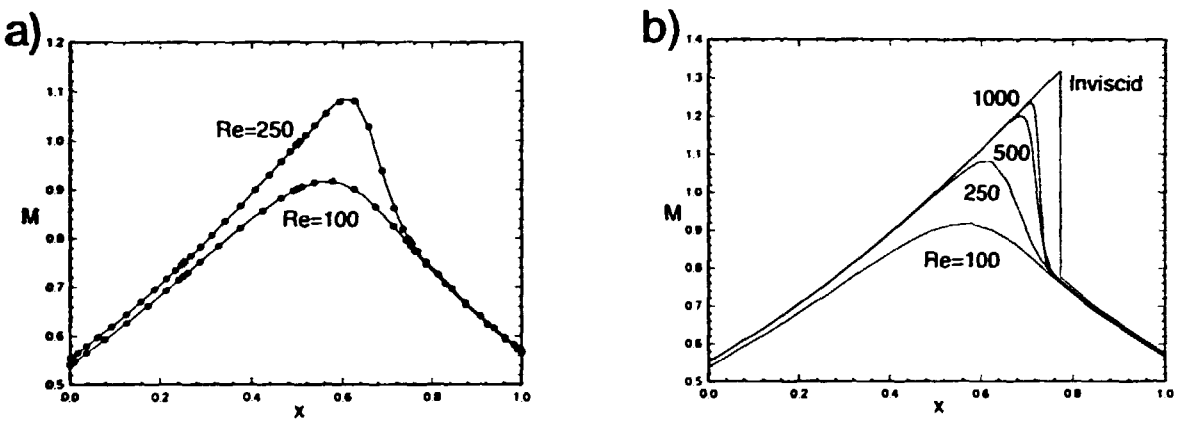

Figure 16. (a) Steady state Mach number profile for viscous, compressible flow through a Laval nozzle at low Reynolds numbers. The full lines illustrate one-domain solutions and the dots illustrate the corresponding four-domain solutions. (b) Steady state Mach number profile for viscous, compressible flow through a Laval nozzle at increasing Reynolds number compared with the inviscid analytic solution. All viscous solutions are obtained as five-domain solutions. For more details see [2].

Work is now in progress to develop the software further in order to allow for addressing compressible viscous flow problems in complex geometries in two and three spatial dimensions.

1) Hesthaven, J.S. and Gottlieb, D., A Stable Penalty Method for the Compressible Navier-Stokes Equations. I. Open Boundary Conditions, SIAM J. Sci. Comp. - accepted for publication.

2) Hesthaven, J.S., A Stable Penalty Method for the Compressible Navier-Stokes Equations. II. One-dimensional Domain Decomposition Schemes, SIAM J. Sci. Comp. - submitted for publication.

3.2.3 A Fast Tau-method for Inverting Rational Variable Coefficient Operators in Bounded Domains

(J.S. Hesthaven, E.A. Coutsias[1], and D. Torres[1] ([1] Department of Mathematics and Statistics. University of New Mexico, USA))

Accurate solution of ordinary and partial differential equations with variable coefficients is of significant importance in all areas of the sciences. Traditionally, such problems are solved by using a finite difference approach in space and/or time. This results in a scheme of low to moderate order, with the error decreasing only as an algebraic function of the grid size in space and/or time. This is true even when applying spectral methods in space for solving time-dependent problems, where the traditional approach is to use some finite difference type integration in time.

The use of spectral methods in bounded geometries for problems where operators need to be inverted has in the past been restricted to only a few special cases, the reason being that the traditional formulation leads to full, nonsymmetric linear problems that are expensive and difficult to solve accurately. We have developed a novel approach, using invertible spectral operators, which results in extremely sparse linear problems; in the simplest case (a two-dimensional linear problem with constant coefficients) a tridiagonal block structure which may be solved either by special purpose direct solvers or by iterative methods, e.g. the method of quasiminimal residuals (QMRs). In our first implementation, the boundary conditions are applied as tau conditions. However, an attractive alternative is to split the solution into its homogeneous and particular part. The former part is then expanded in a basis found as the null-space of the operator, whereas the latter part is approximated by an expansion of an appropriate complete orthogonal basis, e.g. classical orthogonal polynomials, Gegenbauer polynomials, or hypergeometric functions. In this way we obtain that the treatment of the boundary conditions can be done is a numerically stable and efficient way.

The developed algorithm allows for dealing with problems with rational, variable coefficients, be the problem time-dependent or not. We see the future use of this algorithm in two main areas. The scheme allows for performing spectral time integration of ordinary and partial variable coefficient differential equations, thus obtaining schemes with uniform accuracy in time and space. The success of this approach has been confirmed by numerical experiments, where we have been able to obtain spatiotemporal errors of machine accuracy, the wave equation, and advection diffusion problems, hence establishing the method.

An alternative use of the approach is to develop accurate and fast solvers for elliptic problems, which is of significant importance in, e.g., fluid dynamics. By splitting the solution, as described above, we obtain separation of the interior and boundary part of the solution. The use of this approach allows for developing highly accurate and efficient multidomain solvers for elliptic problems, thus enabling us to design a novel multidomain algorithm for solving, e.g., the incompressible Navier-Stokes equations in complex geometries. This aspect is presently being pursued.

3.2.4 Acoustic Eigenmodes in Ducts with Nonuniform Axial Mean Flow

(J.S. Hesthaven, D. Gottlieb (Division of Applied Mathematics, Brown University, USA), and K. Kousen (United Technologies Research Center, East Hartford, USA))

Unlike their uniform counterparts, the linearised Euler equations for unsteady acoustic waves in nonuniform mean flows take the form of variable coefficient differential equations for which no analytic solution is known. However, knowledge about the modal families that may exist under such circumstances is important as they act as the means of communication between various regions of the flow and coupled acoustic elements, e.g. fans in turbines and jet engines. Knowledge about the modal families may also be applied to construct a complete basis set for physically realistic, three-dimensional, far-field boundary conditions for unsteady direct simulation of this type of problems.

We have performed a spatial stability analysis of acoustic waves in ducts. The linearised, isentropic Euler equations for cylindrical and annular ducts containing mean axial shear and swirl components are obtained by assuming an exponential form of the axial, azimuthal, and temporal component. This results in a generalised eigenvalue problem, the solution of which yields the axial wave numbers and radial acoustic eigenmodes of the unsteady problem. The walls of the cylinder are assumed to be either hard or soft with an acoustic liner, modelled by complex impedance.

In order to solve the eigenvalue problem solution with sufficient accuracy we applied a spectral Chebyshev collocation method for spatial discretisation and solved the resulting complex matrix pencil using the QZ-algorithm.

This approach allowed us to identify a new family of eigenmodes with a continuous eigenvalue spectrum related to the nonuniform mean flow. These modes are found to coexist with the discrete modes known from previous analysis of the problem with uniform mean flow. Work is now in progress to use this information to develop a fan-noise prediction system for turbines.

3.2.5 Time-dependent Solution of Viscoelastic Fluid Problems

(Bo Gervang)

When solving time-dependent fluid problems related to industry, we are inevitably confronted with the need for solution of coupled systems of PDEs. An implicit solution of coupled systems at each time step is in most cases not feasible on even the biggest computers today. A decoupling or splitting technique is used where different operators are solved at different stages at each time step.

Solving for non-Newtonian fluid problems and, in particular, problems with viscoelastic fluids we often decouple the stress and momentum equations. Depending on the choice of variables and need of inertia, the momentum equation might further be decoupled into substages. In this study we concentrate on the decoupling between momentum and stress. The momentum operator without inertia, which is used in this study, is the generalised Stokes operator which is of elliptic nature. The generalised Stokes operator is solved fully implicitly, where both direct and iterative methods have been used (see section 3.2.6). The stress equations which are of hyperbolic nature are solved along the characteristics, where the PDEs can be transformed into a set of ODEs. The advantage is a very fast solution technique but spectral accuracy is lost. The accuracy of stress becomes a function of time step and it can be shown that it is second-order accurate in time and that

stability is ensured for all length of time step. Ad hoc methods based on computer experiments are used to determine the time step which ensures stability for the coupled system of momentum and stress equations.

The test problem used in the present study is the flow past a sphere in an infinite expanse of fluid. The dependent variables are expanded in Chebyshev series in the radial direction and in Fourier series in the azimuthal direction.

3.2.6 A Spectral Element Method for the Stokes Problem

(B. Gervang and V.A. Barker (Technical University of Denmark))

We describe a spectral element method for solving the two-dimensional stationary Stokes problem based on the Galerkin technique and equal-order discrete subspaces for velocity and pressure. As shown by Bernardi, Canuto, and Maday[1], this approach produces seven spurious pressure modes in addition to the basis hydrostatic pressure mode and, consequently, the symmetric indefinite coefficient matrix has a rank deficiency of 8. A well-known cure for this is to reduce the order of the discrete pressure subspace.

In this study we examine the consequences of maintaining the equal-order condition and working with the singular system. This procedure is facilitated by knowledge of the null-space of the matrix. The basic steps are the filtering of the right-hand side vector to obtain a consistent system, the solving of this system numerically, and the filtering of the computed pressure to remove the spurious modes.

We make an empirical study of the accuracy of the method and compare it with theory. For certain ranges of computation, the results obtained compare favourably with those published elsewhere based on unequal-order subspaces for velocity and pressure.

1) Bernardi, C., Canuto, C., and Maday, Y. (1986). C.R. Acad. Sci. Paris 303 series I, 971-974.

3.2.7 Accurate Determination of No-slip Solvability Constraints by Recursion Calculations

(E.A. Coutsias (University of New Mexico, USA) and J.P. Lynov)

When calculating solutions to the incompressible Navier-Stokes equations in two dimensions, it is advantageous to work in the vorticity-stream function formulation. Compared with the primitive variable approach, described by velocity and pressure, the vorticity-stream function formulation reduces the number of scalar dynamic equations from two to one, it eliminates the pressure from the calculations, and the incompressibility condition, $\nabla \cdot \mathbf{u} = 0$, is satisfied by construction. However, no-slip boundary conditions leave the Poisson equation, relating the vorticity to the stream function, overdetermined.

We have previously shown[1] how this overdeterminancy can be resolved by imposing solvability constraints on the vorticity field. In particular, we have shown how these constraints can be implemented in spectral algorithms for two-dimensional flows in geometries that are bounded in one direction and periodic in the other, i.e. periodic channel, annulus, and disk geometries. In these cases, the fields are expanded in Fourier-Chebyshev series. For each Fourier mode, the solvability constraints lead to a set of two linear equations for the Chebyshev expansion coefficients of the vorticity field. The constants in these two equations are expressed analytically in terms of Dirichlet Green's functions for the Poisson equation, and they can be determined numerically in a preprocessing step.

It is obvious that precise determination of these solvability constants is essential to the overall accuracy of the calculations. In our previous work, these constants were determined by direct numerical solution of a large number of Poisson equations, one for each combination of Fourier and Chebyshev mode. The numerical values for the constants converge quickly with increasing mode number truncation. However, we were missing a good estimate of the error in the calculations.

In order to resolve this question, we have carried out a more detailed investigation. Analytical expressions for the required Green's functions in the different geometries (channel, annulus, and disk) were obtained, and after some simple calculations only Chebyshev expansions of analytical functions remained. Unfortunately, these expansions converge extremely slowly (quadratically) with increasing mode number, leaving this approach useless.

A different approach was found after deriving a three-term recursion relation between successive solvability constants for increasing Chebyshev mode number and fixed Fourier mode number. Although a direct forward solution following this recursion relation is impossible due to numerical instability, a careful treatment of the three-term difference equation yielded very good results. As a first step in this treatment, both the dominant and the minimal solution to the homogeneous problem[2] are found following a forward and a backward recursion, respectively. Based on these homogeneous solutions, a full solution to the inhomogeneous problem was constructed following the method of variation of constants. The solutions converged rapidly with increasing mode truncation to within machine-order accuracy, and direct error checks show results better than 10^{-13}. Fortunately, comparisons between our new values for the solvability constants and our older ones determined by numerical solution of the many Poisson equations show excellent agreement.

1) Coutsias, E.A. and Lynov, J.P. (1991). Physica D **51**, 482-497.
2) Gautschi, W. (1967). SIAM Review **9**, 24-82.

3.2.8 Pressure Calculation or Two-dimensional Incompressible Flows

(E.A. Coutsias (University of New Mexico, USA), J.S. Hesthaven, and J.P. Lynov)

The accurate calculation of the pressure field in simulations of incompressible flows is of significant importance to applications since it is easily measurable. Although the pressure field evolution must be followed as part of the solution of the problem in the primitive variable formulation, the pressure in the vorticity-stream function formulation of two-dimensional flows is eliminated and, thus, a special treatment is required.

In the velocity-pressure formulation, the pressure is calculated by taking the divergence of the momentum equation and enforcing incompressibility. This approach results in a Poisson equation for the pressure. Unfortunately, it is easy to show that this problem is overdetermined due to the existence of too many boundary conditions. Several approaches have been proposed to resolve this problem, but they all rely on solving a large linear system at each time step and, hence, are very time consuming.

We have followed a different approach which allows for a self-consistent calculation of the pressure distribution from the instantaneous vorticity field in a postprocessing stage.

In the development of the algorithm, special attention was given to accuracy issues by minimising the maximum order of derivatives. As a result, only first-order derivatives enter in the calculation. This is of significant importance to very high resolution spectral simulations of flows.

We have successfully implemented the scheme for a planar channel flow at high

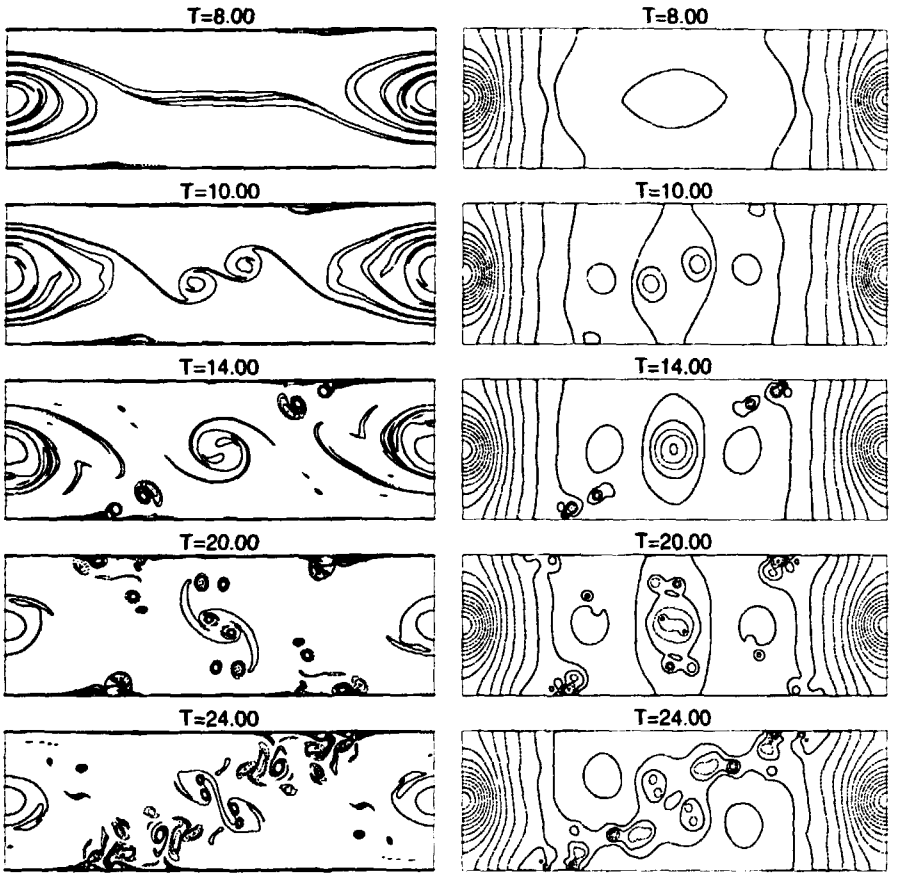

Figure 17. Vorticity (left) and pressure (right) in a plane, incompressible Couette flow at $Re = 40,000$. The full contours show positive values, and the dashed contours negative values.

Reynolds numbers and have calculated the pressure field with a global error of $\mathcal{O}(10^{-7})$. This new approach supplies important new information about the relation between the pressure distribution and the vorticity generation at no-slip walls. An example of the vorticity and pressure fields calculated in a high resolution simulation with 1,024 Fourier modes and 512 Chebyshev modes is shown in Fig. 17.

3.3 Theoretical and Numerical Studies of Nonlinear Processes

3.3.1 Theoretical Estimates of Dipole Trajectories near Circular Cylinders

(E.A. Coutsias (University of New Mexico, USA) and J.P. Lynov)

In connection with our experimental and numerical investigations of the interaction between two-dimensional dipole vortices and circular cylinders, a theoretical estimate of the dipole trajectories was derived. In this estimate, a point vortex model was used for the dipole and free-slip conditions were assumed at the cylinder. The theoretical model produces dipole trajectories for arbitrary dipole strength and injection angle. The trajectories calculated by this simplified model

are in good agreement with the experimental and numerical trajectories, as long as the collision does not involve a strong boundary layer interaction.

3.3.2 Self-organisation in Two-dimensional Circular Shear Layers

(K. Bergeron*, E.A. Coutsias*, J.P. Lynov, and A.H. Nielsen (*University of New Mexico, USA))

Experiments in forced circular shear layers performed in both magnetised plasmas[1,2] and rotating fluids[3] reveal qualitatively similar bifurcation cascades involving states of circular vortex arrangements of varying complexity. These self-organised states have strong influence on the transport properties of the system, a problem that is relevant to fusion experiments as well as to large-scale geophysical flows. We have performed both numerical and asymptotic studies of the Navier-Stokes equations with external forcing in an annular geometry that closely reproduce the experimental observations.

While stable to radially symmetric perturbations at any value of the Reynolds number Re, the steady flow becomes unstable to azimuthal perturbations at a critical value Re_c. There ensues a braid-like arrangement of vortices straddling the forcing region and rotating at constant angular velocity. As Re is increased, these vortices grow like $(Re - Re_c)^{1/2}$ and eventually undergo a symmetry braking transition to a new arrangement of fewer vortices. These transitions are accompanied by clear decreases in both energy and enstrophy of the whole system, as seen in Fig. 18. Further transitions can be observed as well as superpositions of various azimuthal modes with nontrivial temporal behaviour. Linear stability analysis was performed to predict the first transition, and its results were found to be in close agreement with direct simulations of the flow as well as with experimental observations.

1) Pécseli, H.L., Coutsias, E.A., Huld, T., Lynov, J.P., Nielsen, A.H., and Juul Rasmussen, J. (1992). Plasma Phys. Contr. Fusion **34**, 2065-2070.
2) Perrung, A.J. and Fajans, J. (1993). Phys. Fluids A **5**, 493-499.
3) Chomaz, J.M., Rabaut, M., Basdevant, C., and Couder, Y. (1988). J. Fluid Mech. **187**, 115-140.

3.3.3 Investigations of η_i-vortices and Turbulence

(J.P. Lynov, P.K. Michelsen, and J. Juul Rasmussen)

The stability and evolution of perturbed dipolar vortex solutions to a simplified two-dimensional model for the η_i-modes are investigated numerically.

Recently, it has been suggested and indicated from numerical simulations that monopolar and dipolar vortical structures could have strong influence on the dynamics of electrostatic plasma turbulence and on the associated transport in particular. Particles will not solely be transported by small-scale displacements as in diffusion-like processes, but may be trapped by coherent vortices and convected over distances much larger than the vortex scale size. High resolution simulations of, e.g., η_i-turbulence have shown that coherent vortices may develop spontaneously. These had a dominating influence on the evolution of the turbulence, and the associated anomalous transport was found to be significantly reduced as compared with the predictions from quasilinear theory. The existence of coherent vortices in two-dimensional plasma turbulence and their importance to the cross-field particle transport have also been demonstrated experimentally.

Analytical and numerical investigations have recently revealed the existence of

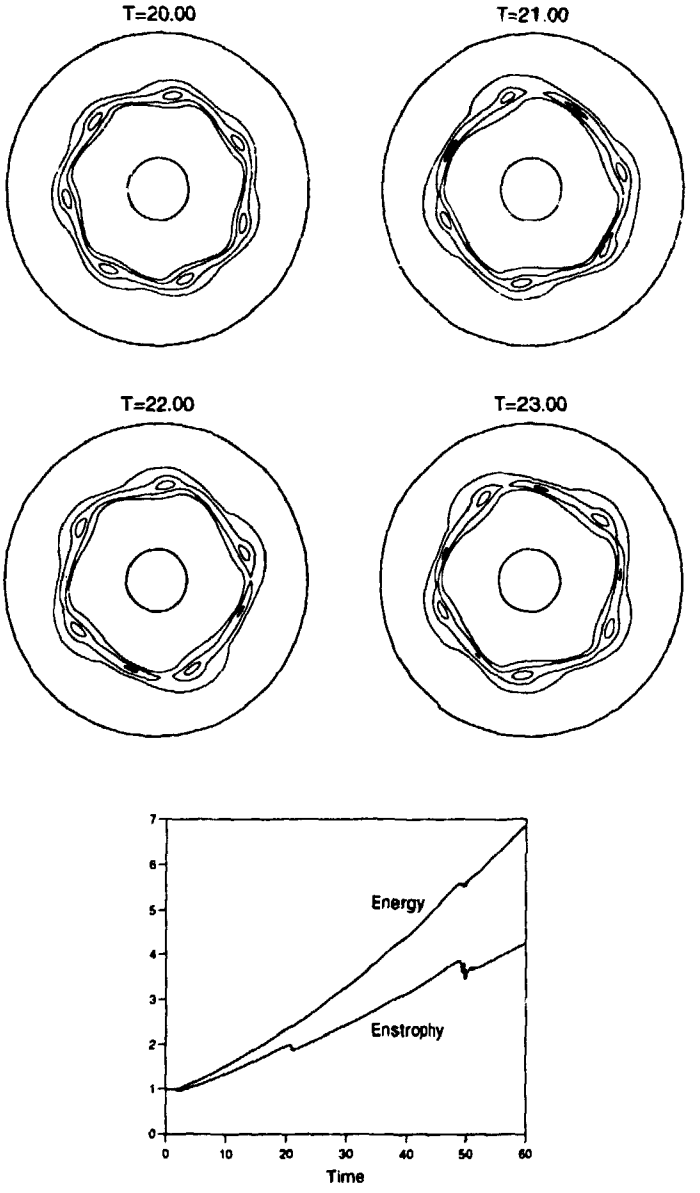

Figure 18. Symmetry breaking bifurcation during gradual speedup. The upper part shows the vorticity field during the transition from mode 7 to 5. The lower part shows the evolution of total energy and enstrophy during the whole speedup phase. The jumps mark the transitions from mode 7 to 5 and from mode 5 to 4.

steadily propagating monopole vortex solutions to the η_i-mode equations. These vortices propagated at velocities outside the phase velocity regime of linear waves. Even in the regime of linearly unstable waves, monopolar vortices were found to propagate and keep their identity for several times their internal turnaround time. Also dipolar vortical structures for the η_i-modes have been found and expressed analytically for simplified η_i-mode model equations. These are only exact solutions when they propagate perpendicularly to the background gradients in density and temperature.

We have performed numerical investigations of the dynamics and stability of these dipolar vortices[1]. In particular, we have investigated the evolution of dipoles that are initially tilted with respect to their preferred direction of propagation. The results show that the gross properties of tilted η_i-dipoles are similar to those

of tilted drift wave dipoles governed by the Hasegawa-Mima equation. When the tilted dipole propagates opposite to the propagation direction of linear waves, its trajectory is gently oscillatory and the dipole keeps its structure. When it is initially propagating in the same direction as the linear waves, it starts a cycloid motion and tends to break up. Finally, we have studied the evolution of cases where the initial condition is set up in k-space with each k-mode chosen randomly in amplitude and phase.

1) Lynov, J.P., Michelsen, P.K., and Rasmussen, J. Juul. Investigations of η_i-Vortices, In: Proceedings of the 1994 International Conference on Plasma Physics **2**, Foz do Iguacu, Brazil, 31 Oct. - 4 Nov. 1994, 91.

3.3.4 Coherent Structures and Transport in Drift-wave Turbulence

(P.K. Michelsen, A.H. Nielsen, T. Sunn Pedersen, and J. Juul Rasmussen)

Large-scale coherent vortex structures may be created spontaneously by self-organisation processes in two-dimensional turbulent flows and play a dominant role in connection with transport of materials in such flows. In magnetised plasmas it has appeared that low frequency electrostatic fluctuations, propagating in a plane perpendicular to the magnetic field, is of great importance to the plasma transport perpendicular to the magnetic field. Such systems are expected to be well described by a two-dimensional approximation. Conventional theories presume that drift wave turbulence is well described by quasi-linear coupling, i.e., a weak coupling between the relevant Fourier modes. However, recent experimental results have indicated the presence of quasi-coherent density and potential structures. Difficulties in developing an approximate edge transport model may be due to oversimplifications which exclude the existence of coherent structures.

A simplified two-dimensional two-field model for drift wave turbulence which couples the fluctuations in the plasma density to those of the plasma potential[1] is investigated analytically and numerically. The system is characterised by three parameters: two viscous damping coefficients and a parameter that determines the degree of adiabatic electron response. The system is studied in the limit of small viscous damping, where the dynamic depends primarily on the adiabaticity parameter. Especially, we investigate structure formation and its relation to transport in drift wave systems.

1) Koniges, A.E., Crotinger, J.A., and Diamond, P.H. (1992). Phys. Fluids **B4**, 2785-2793.

3.3.5 Particle Simulation of Vortical Flow Fields

(A. Høst-Madsen (Dantec Measurement Technology A/S, Skovlunde, Denmark) and A.H. Nielsen)

In close cooperation with Dantec Measurement Technology A/S we have started a particle investigation of two-dimensional flow fields described by the Navier-Stokes equation, see section 3.3.6. The aim of this work is to compare particle image velocimetry (PIV) measurements with exact particle trajectories from computer simulations and - by using PIV on our rotating water tank - to create a "golden triangle" between computer simulations, PIV, and real experiments.

We have developed of spectral code, where the solution of the Navier-Stokes equation can be expanded into a series of orthogonal Fourier modes:

$$\omega(x,y) = \sum_{k_x=-N_x/2}^{N_x/2} \sum_{k_y=-N_y/2}^{N_y/2} \omega_{k_x k_y} \exp(\frac{2\pi i k_x x}{l_x}) \exp(\frac{2\pi i k_y y}{l_y}) \ , \qquad (1)$$

where l_x and l_y are the size of our computational domain, and N_x and N_y are the spectral resolution. The time integration was performed by a fully corrected Adams-Bashforth third-order scheme. As the solution, ω, can be expanded, so can the velocity field. For a particle at a given point, (x, y), we can calculate its velocity with spectral accuracy by performing the series in Eq. 1. Calculating the whole series is very time consuming - 20 particles take as much time as the flow simulation - and as we need in the order of 20000 particles in total, we have implemented the code on a CRAY supercomputer located at UNI*C, Lyngby, Denmark. Up till now we have investigated the flow field from a Lamb dipole, see section 3.3.6, and in the near future we will implement a fully developed turbulent flow field with particles.

3.3.6 The Temporal Evolution of the Lamb Dipole

(A.H. Nielsen, J. Juul Rasmussen, and M.R. Schmidt)

We consider the two-dimensional, unforced, incompressible Navier-Stokes equations in an unbounded domain expressed in the vorticity-stream function formulation:

$$\begin{aligned} \frac{\partial \omega}{\partial t} + [\omega, \psi] &= \nu \nabla^2 \omega \,, \\ \nabla^2 \psi &= -\omega \,, \end{aligned} \tag{1}$$

where $\omega \equiv (\nabla \times \vec{v}) \cdot \hat{z}$ is the scalar vorticity, ψ is the stream function ($\nabla \psi \times \hat{z} \equiv \vec{v}$), and ν is the viscosity. Stationary solutions to Eq. 1 in the absence of viscosity ($\nu = 0$) require that the Jacobian $[\omega, \psi]$ is equal to zero which means that there is a functional relation between the vorticity and stream function, $\omega = f(\psi)$. The most simple dipolar solution with distributed vorticity, and the only one which can be found analytically, is where this function is a linear function: $\omega = \lambda^2 \psi$ inside a circular separatrix and zero outside. This is the well known Lamb dipolar and has the form:

$$\omega = \begin{cases} \frac{2\lambda U_o}{J_0(\lambda R_o)} J_1(\lambda r) & r \leq R_o \\ 0 & r > R_o \,, \end{cases} \tag{2}$$

where U_o and R_o are the speed and radius of the dipole. Please note that for this solution ψ, v_θ, ω, and $\nabla^{2n}\omega$ are all continuous across the separatrix while $\nabla^{2n+1}\omega$ is discontinuous. If we inserted the solution Eq. 2 into Eq. 1, we would end up with a solution of the form: $\omega(\vec{x}, t) = \omega_o(\vec{x}) \exp(-\nu\lambda^2 t)$ which apparently shows that the Lamb dipole is stable also in the viscous case, in the sence that only its amplitude and thereby its speed will decrease, while it will keep its form. But as the solution is not differentiable at the separatrix, the effect of the viscosity is enhanced at the separatrix and tends to smear out the discontinuity in the higher derivatives of ω. A result of this is that the whole structure will expand and since the flow is incompressible, it will trap fluid from outside of the original separatrix. This can be seen in Fig. 19 where we have inserted passive particles in front of the dipole and follow their trajectories while they are convected by the dipole. In Fig. 19a we are only solving the Euler limit of Eq. 1, i.e. no viscosity, and here all the particles are moving past the structures. In Fig. 19b we see the effect of the viscosity as all the particles will become trapped as the structure expands.

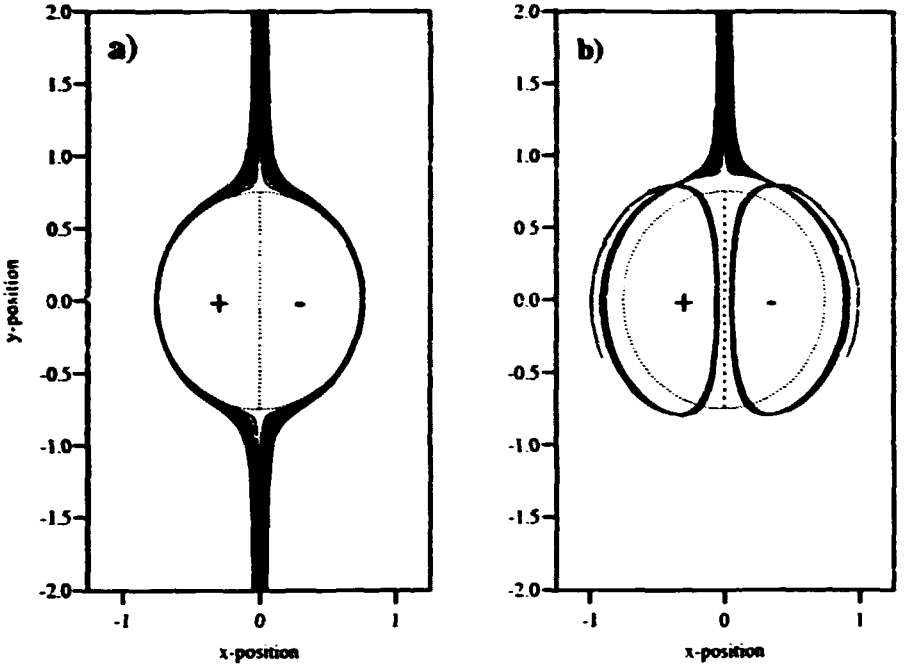

Figure 19. Figure 1. Particle trajectories in the flow field from a Lamb dipole plotted in the frame following the Lamb dipole. The particles were released in the flow field at $y = 2.0$ and in the range $x \in (-0.05; 0.05)$. Figure (a) is for no viscosity while Figure (b) is with high viscosity. The dashed line denotes the separatrix at $T = 0$.

3.3.7 Formation of Dipolar Vortices by Self-organisation in Two-dimensional Flows

(A.H. Nielsen, J. Juul Rasmussen, and M.R. Schmidt)

The formation of dipolar vortices from localised forcing in a two-dimensional flow is investigated theoretically and by direct numerical solutions of the two-dimensional Navier-Stokes equations.

When the initial condition consists of two nearby vortices with Gaussian stream function and opposite vorticity, we observe the formation of a Lamb-type dipolar vortex, characterised by a near linear functional relationship between the stream function and the vorticity (see section 3.3.6). For distances between the centres of the initial vortices larger than a critical value measured in terms of the radii of the initial vortices, no dipolar vortex is formed. These results compare qualitatively with experimental results of dipole vortex generation in stratified fluids by van Heijst and coworkers at Eindhoven University of Technology[1]. A detailed quantitative comparison is in progress.

We have also investigated the formation of dipolar vortices by self-organisation of a localised turbulent patch. The patch is characterised by its energy and enstrophy and has a net linear momentum, but no net circulation. It is constructed from fluctuations with random phases and an isotropic energy spectrum, $\propto \exp(-(k - k_0)^2/\Delta^2)$; the localisation of the patch is provided by multiplying this wave field by $\exp(-r^4/r_0^4)$ in configuration space, after a sinusoidal in x has been added to provide a finite linear momentum, P_y, in the y direction. The resulting development is shown in Fig. 20. We observe a clear self-organisation of the patch into a propagating dipolar structure. This development is qualitatively described as a self-organisation in a viscid flow. Using the fact that the enstrophy, W, decays

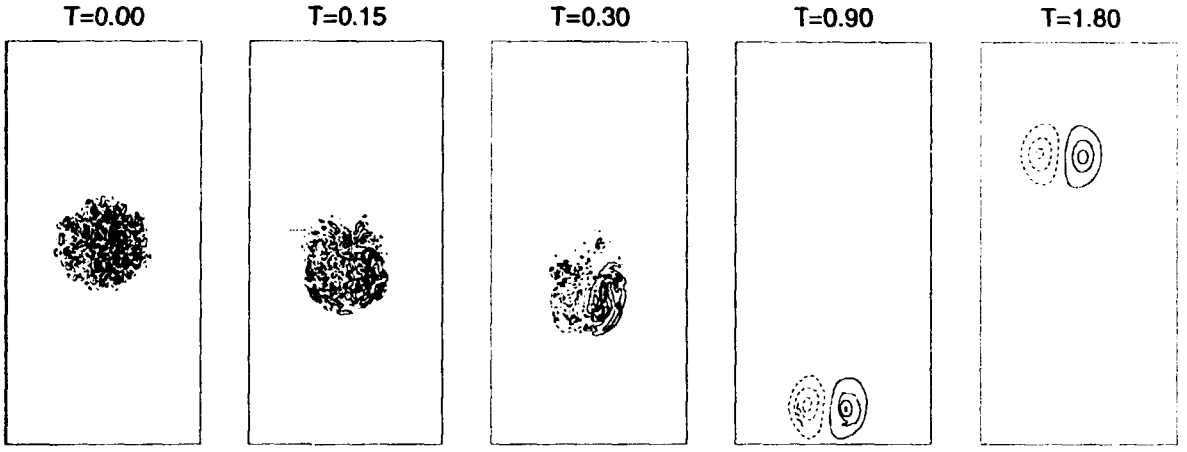

Figure 20. Evolution of a turbulent patch with initial linear momentum into a dipolar structure. The parameters are $k_0 = 20$, $\Delta = 10$, *and* $r_0 = 0.20$. *Initially,* $E = 0.314$, $W = 162$, *and* $P_y = 0.34$. *The resolution is* $N_x = N_y = 128$.

faster than the energy, E, we have looked for solutions that minimise W under the constraint of a fixed E and a fixed linear momentum following the idea of Leith[2].

1) Flor, J.B. and van Heijst, G.J.F. (1994). J. Fluid Mech. **279**, 101-133.
2) Leith, C.E. (1984). Phys. Fluids **27**, 1388-1395.

3.3.8 Instability of Two-dimensional Solitons and Vortices in Defocusing Media

(E.A. Kuznetsov (Landau Institute for Theoretical Physics, Moscow, Russia) and J. Juul Rasmussen)

The stability of two-dimensional soliton and vortex solutions to the nonlinear Schrödinger equation (NLSE) with repulsion is considered. This equation which reads:

$$i\psi_t + \frac{1}{2}\nabla^2\psi + (1 - |\psi|^2) = 0 \qquad (1)$$

has several important applications. In the context of nonlinear optics it describes the nonlinear propagation of electromagnetic waves in a defocusing medium, i.e., in a Kerr medium where the refractive index decreases with the wave intensity. Equation (1) has also been employed as a model for the dynamics of a weakly imperfect Bose gas, where ψ takes the role as the condensate wave function. For both of these cases two-dimensional soliton and topological vortex solutions have been investigated both theoretically and numericaliy.

We have investigated the stability of the whole family of these two-dimensional solutions with respect to three-dimensional perturbations are in the framework of Eq. (1). We found that the structures are in general unstable with respect to long wavelength symmetric perturbations, while they appear to be stable with respect to antisymmetric perturbations. In the limit where these soliton solutions have large velocities ($v \to C_s$, where C_s is the "sound" velocity, the minimum phase velocity of linear waves), the instability is analogous to the instability of one-dimensional acoustic solitons in a medium with positive dispersion as described by the Kadomtsev-Petviasvili equation. For smaller velocities the structure appears as a dipolar vortex and here the instability becomes similar to the so-called Crow instability of two vortex filaments with opposite circulations in hydrodynamics

as described in terms of the Euler equations. It is conjectured that the nonlinear evolution of this instability will lead to a reconnection of the vortex filaments and to the formation of vortex rings.

3.3.9 Two-dimensional Dynamics in Discrete Nonlinear Schrödinger Equation in the Presence of Point Defects

(V.K. Mezentsev (Institute of Automation and Electrometry, Novosibirsk, Russia), P.L. Christiansen*, Yu. B. Gadiclei (Institute of Theoretical Physics, Kiev, Ukraine), J. Juul Rasmussen, and K.Ø. Rasmussen* (*IMM, The Technical University of Denmark))

Recent progress in investigations of discrete systems has highlighted the rich variety of essentially discrete phenomena that have no analogues in the corresponding continuous limits[1,2]. Another reason for the general interest in discrete models is that they often provide more natural descriptions of real processes than their particular continuous limits. Of special effect in discrete systems one may mention the stable stationary narrow solitons[2] and the breather-like postcollapse evolution of contracted pulses[1].

We considered the discrete nonlinear Schrödinger equation, which is the most general model of coupled nonlinear oscillators in two dimensions:

$$i\frac{\partial U_{n,m}}{\partial t} + U_{n+1,m} + U_{n-1,m} + U_{n,m+1} + U_{n,m-1} - \omega_{n,m}U_{n,m} + 2|U_{n,m}|^2 U_{n,m} = 0.$$

Usually, the oscillators are treated to be equal, i.e. they have the same linear frequency $\omega_{mn} = \omega_0 = \text{const}$. This model contains the effects of linear coupling with the nearest neighbours and intrinsic nonlinearity.

Numerically, we have found new moving stable structures which demonstrate solitary wave propagation for a long time. Particular attention was paid to the presence of point defects and their role in the nonlinear dynamics. The defect is modelled by giving a certain site its own specific linear frequency. First, we found a new family of narrow solitons which are connected to the point defects. Then, we studied the nonlinear interaction between moving solitons and standing narrow states of both types (ordinary solitons and the solitons introduced by the defect). We also found that the point defects play a significant role in quasi-collapse dynamics.

1) Bang, O., Rasmussen, J.J., and Christiansen, P.L. (1993). Nonlinearity 7, 205.
2) Mezentsev, V.K., Musher, S.L., Ryzhenkova, I.V., and Turitsyn, S.K. (1994). Pis'ma v ZhETF. (JETP Letters). Accepted for publication.

3.3.10 Higher Order Nonlinear Schrödinger Equations in Continuum Physics

(J. Wyller (Narvik Institute of Technology, Norway), T. Flå (University of Tromsø, Norway), and J. Juul Rasmussen)

Under a slowly varying amplitude assumption, the modulation of small, but finite amplitude wave trains in one dimension is described by a Schrödinger type of equation with a cubic nonlinearity. In dielectric guides, for example, the nonlinearity describes the Kerr effect. The higher order nonlinear Schrödinger equation (HNLS-equation):

$$i\phi_\tau + \phi_{\xi\xi} = a_1|\phi|^2\phi + a_2|\phi|^4\phi + ia_3|\phi|^2\phi_\xi + (a_4 + ia_5)\phi(|\phi|^2)_\xi \quad (1)$$

and ξ the reduced time coordinate, both being normalised to true physical quantities. In this context, the nonlinear terms represent: the Kerr effect ($a_1|\phi|^2\phi$), the first-order contribution to the nonlinear saturation ($a_2|\phi|^4\phi$), the nonlinear dispersion ($ia_3|\phi|^2\phi_\xi$ and $ia_5(|\phi|^2)_\xi\phi$,), and the Raman effect ($a_4(|\phi|^2)_\xi\phi$). In addition to optical phenomena, Eq. (1) with $a_4 = 0$ is a model for the so-called marginally stable modulated wave trains in different physical systems.

When $a_3 \neq 0$, Eq. (1) can be transformed to the following extended derivative nonlinear Schrödinger equation:

$$q_t + iq_{xx} + |q|^2 q_x + i\gamma(|q|^2)_x q + i\sigma|q|^4 q = 0 \tag{2}$$

by means of a point transformation and a subsequent gauge transformation. Here γ is proportional to a_4 and σ is a function of a_1, a_2, a_3, and a_5. The properties of this equation are summarised as follows:

- When $\gamma = \sigma = 0$, Eq. (2) is completely integrable and can be solved by means of the inverse scattering transform. The soliton solutions represent self-phase modulated wave packets.
- When $\gamma = 0$, Eq. (2) is a Hamiltonian system possessing three conservation laws (i.e. conservation of action, momentum, and energy). A detailed study of Eq. (2) with respect to cnoidal waves, linear and nonlinear stages of the modulational instability and recurrence has been carried out by Flå and Wyller[1]. The instability criterion reads $k_0 > -2\sigma q_0^2$, where k_0 and q_0 are carrier wave number and amplitude, respectively, of the plane wave solution to Eq. (2).
- When $\gamma \neq 0$, $\sigma \neq 0$, only the action density is conserved. The plane wave solutions of Eq. (2) are modulationally unstable in all regimes of the carrier wave number k_0 and amplitude q_0. The periodic cnoidal waves, which exist in the case $\gamma = 0$, are destroyed by the Raman term $i\gamma(|q|^2)_x q$
- Equation (2) possesses group invariant solutions of the self-similar type for all combinations of σ and γ.

1) Flå, T. and Wyller, J. (1993). Physica Scripta **47**, 214.

3.3.11 Defocusing Solutions of the Hyperbolic Nonlinear Schrödinger Equation

(L. Bergé (Commissariat à l'Energie Atomique, CELV, France) and J. Juul Rasmussen)

The elliptic/hyperbolic nonlinear Schrödinger equation

$$iu_t + u_{rr} + (d-1)u_r/r + su_{zz} + |u|^2 u = 0 \tag{1}$$

is the canonical equation that governs the propagation of the envelope $u(r, z, t)$ of an almost monochromatic, weakly nonlinear packet of dispersive waves. It arises in a wide variety of contexts, such as plasma physics and nonlinear optics when the transverse (r-plane of dimension number d) distribution of a high frequency carrier wave is modulated by slow-frequency motions as the wave propagates along the longitudinal z-axis.

By means of a Lagrangian approach, $d = 1$ solutions were recently described in both situations of so-called anomalous and normal dispersions corresponding to the elliptic/hyperbolic values $s = +1$ and $s = -1$, respectively[1]: it was shown that when $s = +1$, an anisotropically-shaped localised structure having a negative energy tends to collapse in a finite time with an identical contraction rate in both transverse and longitudinal directions, while in the opposite case when $s = -1$, the waveform asymptotically defocuses with a linear-in-time dilation rate. Even

energy tends to collapse in a finite time with an identical contraction rate in both transverse and longitudinal directions, while in the opposite case when $s = -1$, the waveform asymptotically defocuses with a linear-in-time dilation rate. Even though these results remain in good agreement with various numerical results, the global behaviour of $u(r, z, t)$ in the presence of normal dispersion has never been examined from a mathematical point of view in the past. The present work therefore consists in establishing rigorous estimates based upon some concavity arguments: they prove that the solution $u(r, z, t,)$ - initially localised in space - spreads out in time for $s = -1$, at least in the following situations:

(i) In the two-dimensional case ($d = 1$); if the initial velocity of the structure defined along the z-axis is strictly positive, then the wave packet disperses along this axis in a finite time. For all other initial data, the wave surely spreads out as t tends to infinity, and the transverse size of the structure never tends to zero even when its energy is negative, unlike the $s = +1$ case;

(ii) In the three-dimensional case ($d = 2$), a positive energy wave packet also disperses in a finite time when the initial velocity of the solution is strictly positive along the longitudinal axis, and asymptotically defocuses for different initial velocities. The fate of a three-dimensional structure evolving with a negative energy in a normal dispersive medium, however, remains under investigation.

(iii) Besides, no nonzero localised stationary solution exists whatever the space dimension number d may be.

Finally, resulting from a perturbative analysis performed around the stationary ground state of Eq. (1) defined for $s = 0$ and $d = 2$, the salient difference between both cases, $s = +1$ and $s = -1$, is that a z-periodic perturbation induces a local self-concentration of the ground state mass in the first situation (which can ultimately lead to the collapse), whereas in the second situation the same mass tends to disperse along the z-axis, hereby reflecting the delocalising dynamics summarised above.

1) Bergé, L. (1994). Phys. Lett. A 189, 290-298.

3.3.12 Vortex Merger in the Presence of Free Surface in Rotating Fluids

(X. He (also CATS, Niels Bohr Institute, University of Copenhagen, Denmark) and J. Juul Rasmussen)

Using a probabilistic method, we present a functional critical separation distance d_c for two circular patches unequal in vorticity and radius, in the presence of a free surface due to background rotation. We first impose two forces on the vortices: one is internal local strain $F_i = -\omega_1 R_1^2/(r\delta)$, the other is external background rotation $F_e = r^2 f^2/\Gamma$, where f corresponds to the Coriolis parameter in rotating fluids. We then seek for the most likely probability of finding the two vortex centres separated over a distance r, from which the critical distance d_c is derived by using the geometrical argument and defining the merger criterion for the small vortex. We show that in the case of an identical vortex pair, a pair with the same sign vorticity as the background rotation (cyclones) has larger critical distances than a pair with opposite sign to the background rotation (anticyclones). The result is quantitatively in agreement with the observations in a rotating tank, and supports the explanation in a numerical simulation for the anomalous vortex merger.

3.4 Experimental Studies of Nonlinear Processes

3.4.1 Pattern Formation in Bacteriorhodopsin Thin Films

(M. Saffman and J. Glückstad)

The formation of regular structures and patterns in initially homogeneous media is a central topic in modern nonlinear dynamics. Pattern formation has been observed and studied in a wide variety of systems including fluids, chemical reactions, nonlinear optics, and synthetic nonlinear devices. There is at present much interest in pattern formation in optical systems from both fundamental and applied perspectives. The fundamental interest in pattern formation centres on understanding the mechanisms that select the observed patterns and control their dynamic stability, or lack thereof. Optical pattern formation can also form the basis of dynamic systems that process information optically[1]. The possibility of generating very small-scale patterns, in the order of a wavelength, is also potentially relevant to optical data storage.

We have studied, both experimentally and theoretically, the formation of patterns in thin films of the nonlinear material bacteriorhodopsin[2]. The geometry of a thin nonlinear film with feedback mirror was used as shown in Fig. 21. The nonlinear transverse phase shift due to the bacteriorhodopsin film is converted into a transverse amplitude modulation by the free space propagation. The amplitude modulation then further affects the nonlinear phase shift, and the resulting steady state mode has the form of a multilobed structure as shown in Fig. 22.

Previous theoretical work on pattern formation in thin films has centred on Kerr type media where the nonlinearity is purely dispersive. Bacteriorhodopsin, on the other hand, is characterised by a mixed absorptive-dispersive nonlinearity. A theoretical model of pattern formation in this type of material has been developed and used to predict analytically the threshold intensity necessary for the observation of transverse spatial patterns. The theoretical prediction corresponds well to the experimentally observed threshold level.

1) Saffman, M. "Dynamisk optisk informationsbehandling i fotorefraktive kredsløb" (1994). DOPS-NYT (News of the Danish Optical Society) 9, No. 4, 15-20 (in Danish).

2) Glückstad, J. and Saffman, M. "Spontaneous Pattern Formation in a Thin Film of Bacteriorhodopsin with Mixed Absorptive-dispersive Nonlinearity, to appear in Opt. Lett., 1995.

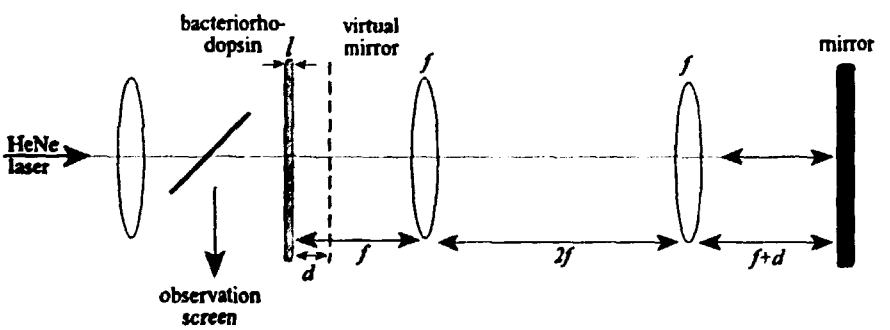

Figure 21. Experimental geometry. The light source is a 30 mW HeNe laser. The virtual mirror based on a 4f lens system with real mirror allows small mirror spacings d to be investigated conveniently.

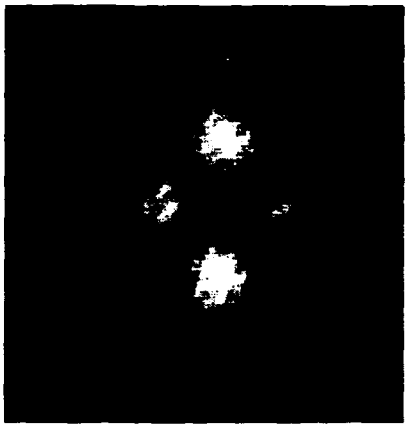

Figure 22. A typical transverse structure, observed with $d = 3$ mm.

3.4.2 A Parabolic Vessel for Investigations of Vortices and Shear Flows on the Beta-plane

(M.O. Nielsen, B. Stenum, J. Juul Rasmussen, E.N. Snezhkin, and M.V. Nezlin (Kurchatov Institute, Moscow, Russia))

For the investigations of vortices and shear flow instabilities in inhomogeneous rotating flows with a varying Coriolis force we have constructed a parabolic vessel. The free surface of a fluid rotating in a gravitational field at a constant angular velocity around the vertical axis assumes a parabolic shape. If the fluid is contained in a rotating vessel with a bottom of an approximate parabolic form, the fluid may have a constant depth. When the depth is small enough for the shallow water approximation to be valid, the rotating fluid serves as a model of the oceans or atmospheres on rotating planets[1)], where the Coriolis force varies from its maximum value at the poles to zero at the equator. In the parabolic vessel the Coriolis force is maximum at the "bottom" of the parabola and decreases along the radius. The dynamics in such a system is furthermore similar to the low frequency dynamics in a magnetised plasma with a density gradient perpendicular to the magnetic field. The two cases are in a first approximation (i.e. the beta-plane approximation, where the Coriolis force is assumed to vary linearly, and for the plasma case the density profile is exponential) modelled with the same evolution equation.

The setup with the parabolic vessel is shown schematically in Fig. 23. The inner diameter of the vessel at the top is 56 cm and its focal length is 8.6 cm. It is designed to a rotation rate of around 72 rpm, and at that speed a water layer of 1 cm depth has approximately constant thickness. The Rossby radius, which is a characteristic scale size for vortices and waves (Rossby waves), is with these parameters around 2.6 cm. The inner part (the pole part with radius 10 cm) of the paraboloid may be rotated independently and, thus, a velocity shear can be formed. A water circulation system makes it possible to force a flow from the outer periphery of the paraboloid to the centre (and also in the opposite direction), which on a rotating planet would correspond to a meridional flow. The whole setup is surveyed by a video camera mounted in the rotating system and connected to the equipment in the laboratory via slip rings. Several diagnostic methods are planned to be employed, where one of them is based on the depth measuring system described in section 3.4.3. Vortices will show up as a local increase of the fluid layer thickness for anticyclones (i.e. vortices with internal rotation opposite

to the bulk rotation of the fluid) or as a decrease in the thickness for cyclones (which have internal rotation in the same direction as the bulk rotation).

Several experiments are planned for the rotating vessel. First, the dynamics of individual vortices will be examined; these vortices may be excited either by locally adding some fluid resulting in anticyclones, or by locally sucking out some fluid resulting in cyclones. Then, we will investigate the formation of vortices by the shear flow instability and also the influence of the beta-effect on the shear flow instabilities. Furthermore, we plan detailed investigations of the effects of the varying Coriolis force on the flow dynamics when fluid is forced to flow from the outer periphery of the vessel toward the pole part, and we will also examine the effects of the shear layer on this flow.

1) Nezlin, M.V. and Snezhkin, E.N. (1993). *Rossby Vortices, Spiral Structures, Solitons*. Springer-Verlag Berlin Heidelberg.

3.4.3 Depth Measurements in Rotating Parabolic Vessel

(T. Stoltze Laursen, F. Okkels, J. Juul Rasmussen, E.N. Snezhkin (Kurchatov Institute, Moscow, Russia), and B. Stenum)

A depth measuring technique is being developed for the parabolic vessel (see section 3.4.2) in order to measure depressions/elevations of the surface caused by small waves and vortices. The technique is based on emission of light from water containing fluorescent dye. The water is illuminated with UV light (wavelength approx. 365 nm). The emitted intensity I will be a function of the instantaneous water depth h. The emission law is $I = I_0\ (1 - \exp(-h/\tau))$, I_0 being the emitted intensity for infinite depths and τ a penetration depth. The system comprises a video source (camera/VTR), a PC with framegrabber board and sufficient disk storage. The free water surface is viewed from above, pictures of the whole field are captured, and the intensities are stored on disk in grey-scale intensities. The system is calibrated in order to determine the emission depth and the penetration depth in each pixel (calibration constants) of the captured picture, the water depth h is evaluated as a function of the emitted intensity I for each pixel in the picture. All data processing software is written in C under Windows. The method has been tested in a test setup (mean water depth approx. 15 mm), the accuracy of the measured water depth h was within 0.1 mm in the calibration pictures. Excited waves were easily detected as illustrated in Fig. 24.

3.4.4 Wall Induced Collapse of 2D Dipolar Structures

(T. Stoltze Laursen, J. Juul Rasmussen, E.N. Snezhkin (Kurchatov Institute, Moscow, Russia), and B. Stenum)

An initially 2D dipolar structure is formed by an inlet flow occurring in a uniform gap between two parallel walls, where the length of the gap is limited to the sides by two parallel side walls[1]. The Reynolds number of the inlet flow is approximately: $Re = Ud/\eta = 280$ (U being the cross sectional average velocity, d the gap width, and η the kinematic viscosity). The inlet takes place during a period of $\Delta t^* = \Delta t U/d = 2.7$($\Delta t$ being the duration of the flow). Two small nozzles for dye injection were placed on the outside of the inlet, one nozzle in the mid plane between the two side walls, the other close to the left side wall. Before each test, dye - with a density slightly larger than the density of the water - was injected forming vertical strings in the resting fluid. When the dipole is formed, some dye is trapped in one of the two vortices forming the dipole, thereby visualising the

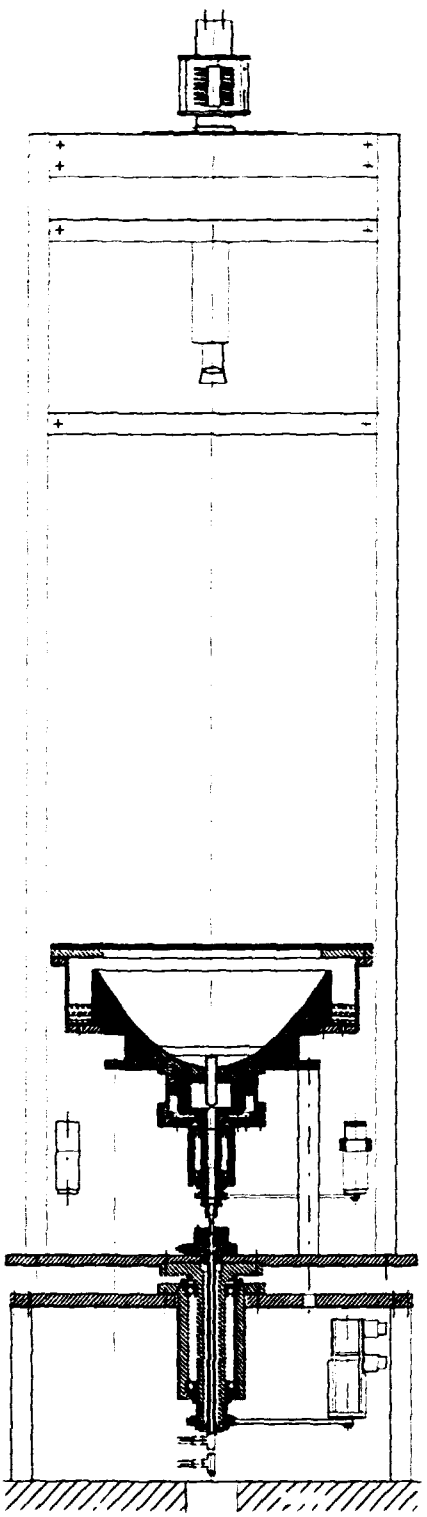

Figure 23. The parabolic vessel.

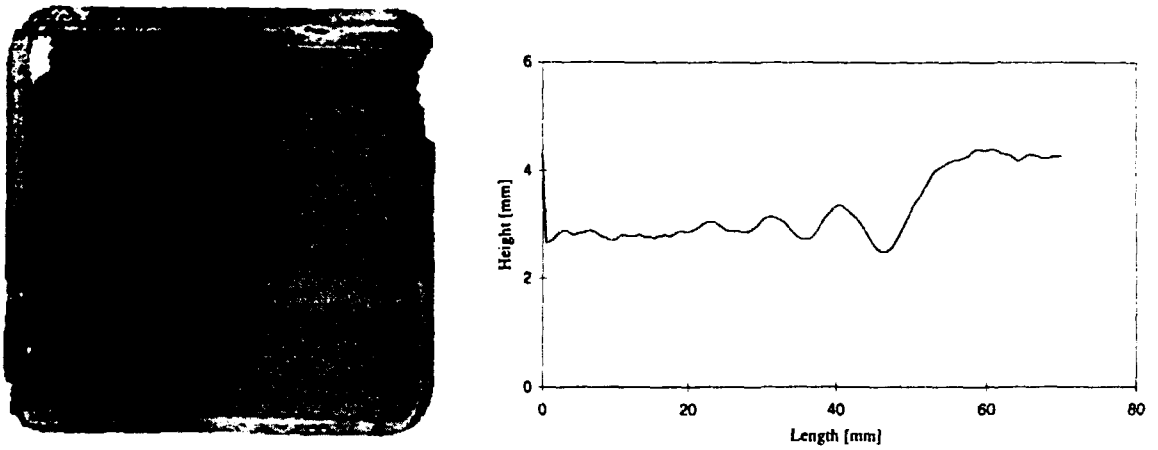

Figure 24. (a) Picture showing waves in a test vessel. Depths are shown as grey scales. b) Typical wave profile from waves shown in (a).

flow. As indicated in Fig. 25, the dye trace from the central dye nozzle shows no sign of asymmetries; the structure appears to be 2D at this position. The dye trace from the side nozzle shows a velocity in the core region of the vortex perpendicular to the wall directed away from the wall, indicating a spiral motion and the existence of a Burgers vortex. Finally, the dye is dispersed indicating a breakup of the vortex structure. The core region velocity is believed to be a boundary layer effect from the side walls analogous to the von Karman viscous pump. Time series of 2D vector maps can be produced by means of particle tracking (Digimage flow diagnostic system). Measurements of this kind indicate that the flow structure, which was initially 2D, eventually breaks up and becomes a true 3D structure. It is believed that a vortex ring is formed through wall induced reconnection of the dipolar structure.

1) Homa J., Lucas, M., and Rockwell, D. J. Fluid Mech. **197**, 571-594.

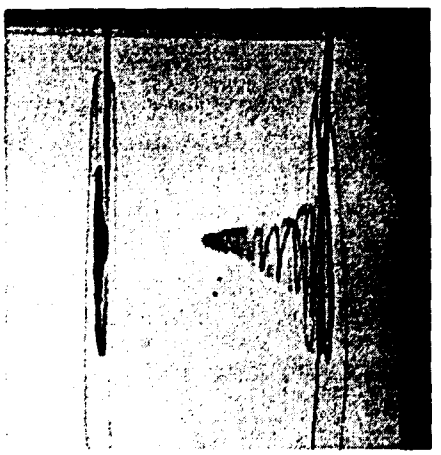

Figure 25. Dye traces showing the wall induced core velocities directed away from the wall.

3.4.5 Whole Field Velocity Measurements of Vortex Rings

(T. Stoltze Laursen, D.R. McCluskey (Dantec Measurement Technology A/S), J. Juul Rasmussen, and B. Stenum)

A new particle image velocimetry (PIV) diagnostic system has been introduced by Dantec Measurement Technology (FlowMap). The system has been tested by measuring velocity fields in a vertical cut of horizontally ejected vortex rings. This is a well known case that has been studied both theoretically and experimentally for more than one century. Vortex rings can be produced with a wide range of flow parameters.

For the present studies the vortex rings were produced by inlet of well defined water puffs through a circular tube with an inner diameter of 4.7 cm in a water tank of a length of 80 cm, a width of 50 cm, and a depth of 50 cm. The water puff was simply produced by gravity induced inlet of a water column through a 90 degrees bending by means of a timer controlled valve connecting the air inside the tube to the outside via an air flow resister consisting of a small tube with an inner diameter of 2 mm. The vortex rings can be visualised by adding fluorescence dye to the water inside the tube and illuminating by a light sheet produced by means of a light projector. The evolution of a vortex ring is shown in Fig. 26. From the dye studies some characteristic parameters such as propagation speed and azimuthal velocity inside the ring have been determined and compared with the values obtained with the Dantec system. The FlowMap system is based on a fast correlation analysis of multiple exposed videoimages of the flow seeded with pollen and illuminated by a pulsed light sheet produced by an argon ion laser and a polygon scanner. The flow fields measured with the Dantec system have shown good agreement with the dye studies as well as with flow fields measured by particle tracking (DigImage) by which similar videoimages could be analysed.

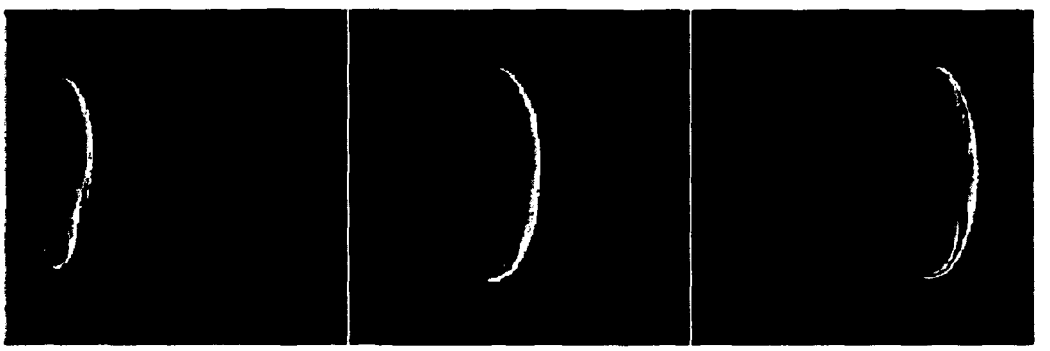

Figure 26. The evolution of a vortex ring visualised by fluorescent dye.

3.4.6 Damping of a Vortex Ring in a Stratified Fluid

(R. de Nijs (Eindhoven University of Technology, the Netherlands), T. Stolze Laursen, J. Juul Rasmussen, and B. Stenum)

The transition from a 3D vortex ring structure to a 2D dipole structure has been studied for a vortex ring ejected horizontally in a stratified fluid.

The vortex rings were produced by gravity induced inlet of well defined water puffs through a circular tube with an inner diameter of 4.7 cm in a water tank of a

length of 80 cm, a width of 30 cm, and a depth of 60 cm. In order to characterise the initial conditions, vortex rings ejected in a homogeneous fluid have been carefully studied by means of both dye visualisation and particle tracking. The stratified fluids were produced by the two-tank method. In stratified fluids the vertical motion in the vortex ring is damped by the stratification, and energy is radiated away from the vortex ring via internal waves. For the dye studies this damping is seen as a reduction of the size of the vortex ring. After propagating some distance depending on the initial energy of the vortex ring and the strength of stratification the vortex ring collapses into a horizontal motion and subsequently a plane dipole is formed. This dipole continues to propagate horizontally at a velocity much less than that of the initial vortex ring. The formation of the dipole seems to be similar to that experienced after injection of a turbulent jet in a stratified fluid[1)].

1) van Heijst, G.J.F. and Flor, J.B. (1989). Nature **340**, No. 6230, 212.

3.5 Plasma Theory and Diagnostics

3.5.1 Magnetic Stresses in Ideal MHD Plasmas

(V.O. Jensen)

A comprehensive study of the advantages of using magnetic stresses for determining steady state equilibria of ideal MHD plasmas has been undertaken. The basic equations are:

$$\text{the force density equation,} \quad \mathbf{j} \times \mathbf{B} = \nabla p \tag{1}$$

$$\text{the Maxwell equations,} \nabla \times \mathbf{B} = \mu_o j \quad \text{and} \nabla \cdot \mathbf{B} = 0\,. \tag{2}$$

It is shown that the resulting stresses acting on an area element, ds, in a magnetised plasma comprise:

- A shear stress, $B_{\|} B \perp / \mu_o$, acting along the projection of the **B**-lines on ds.
- A tensile stress, $B_{\perp}^2/\mu_o$, acting perpendicular to ds.
- A compressive stress, $B^2/2\mu_o$, acting perpendicular to ds.
- A particle pressure, p, acting perpendicular to ds.

The stresses are used to derive and explain various properties of magnetically confined plasmas.

3.5.2 Optical Plasma Diagnostics

(M. Saffman, L. Lading, S.G. Hanson, T.M. Jørgensen, and R.V. Edwards (Case Western Reserve University, Cleveland, USA))

Despite many years of intensive research and development towards the use of magnetically confined plasmas for the production of energy, much remains unknown about the basic physical processes inside the plasma. There is an ongoing need for the development of new diagnostic techniques that allow detailed measurements to be performed, without disturbing the plasma. Within the framework of Risø's association with EURATOM, we are developing a time-of-flight type laser anemometer for measurements of electron density fluctuations in plasmas. The Doppler type laser anemometer, where the velocity is found from measuring the differential Doppler shift of light scattered from a pair of crossed beams, has for many years been used for measurements of plasma turbulence. These measurements are plagued, however, by very poor spatial resolution along the beams due

to the small scattering angles that are necessary for measurements of turbulence of long wavelength. In order to correct this deficiency we have proposed using a time-of-flight type configuration for plasma measurements[1]. The tightly focussed beams of the time-of-flight anemometer result in a great improvement in the axial resolution, without sacrificing accuracy in the velocity measurement. In order to have sufficient sensitivity to measure the weak phase perturbations encountered in plasmas, it is necessary to work with a reference beam configuration. The resulting system is a hybrid combination of the Doppler and time-of-flight approaches. An interesting byproduct of this work is that the hybrid design may be superior to existing laser anemometers. An information theoretic analysis[2] shows that in principle it has a much lower measurement uncertainty than either the Doppler or the time-of-flight approaches.

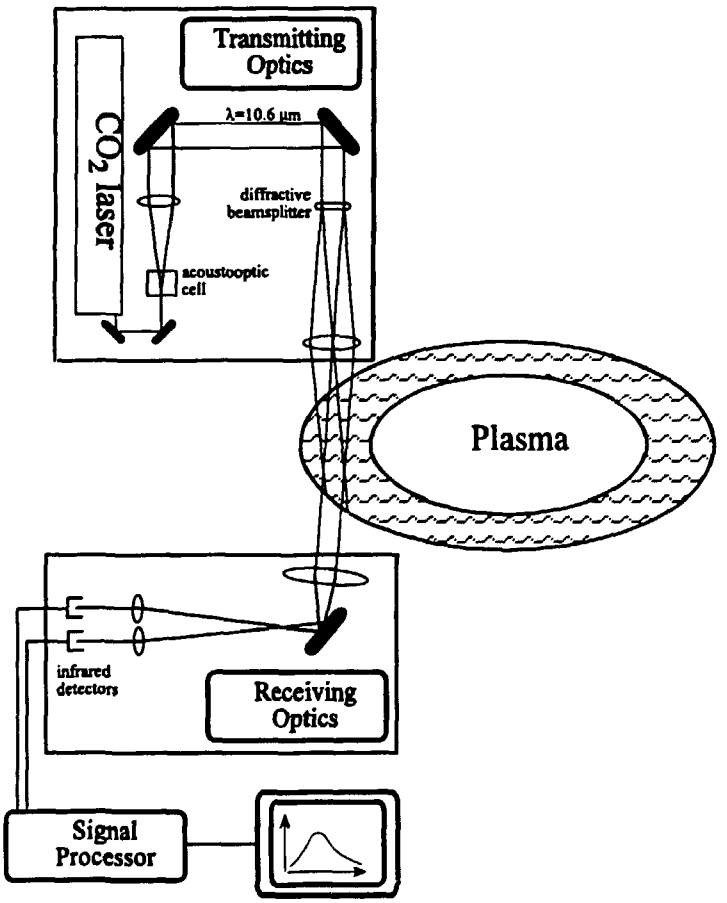

Figure 27. Generic layout of a light scattering diagnostic for measurement of plasma density fluctuations.

The generic layout of such a scattering experiment is shown in Fig. 27. An 80 W cw CO_2 laser operating at 10.6 mm is split into four beams using an acousto-optic cell together with a specially fabricated ZnSe diffractive element. The infrared detectors are liquid nitrogen cooled HgCdTe photoconductors. This system is currently being tested at Risø using a turbulent air jet. It is planned, upon successful completion of these tests, to move the system to the Wendelstein VII-A stellerator at the Max Planck Institute for Plasma Physics in Garching, for measurements on a large-scale plasma device.

1) Lading, L., Saffman, M., Hanson, S.G., and Edwards, R.V. "A Combined Doppler and Time-of-flight Laser Anemometer for Measurement of Density Fluc-

tuations in Plasmas", submitted to The Journal of Atmospheric and Terrestrial Physics, June 1994.
2) Saffman M. and Jørgensen, T.M "On the Optimum Spatial Code of a Laser Anemometer", submitted to Opt. Comm., December 1994.

4 Pellet Injectors for Fusion Experiments

4.1 Introduction

Injection of frozen hydrogen or deuterium pellets is an essential part of several plasma fusion experiments. Risø has developed a system for this type of pellet injection. The department has offered to build injectors for fusion experiments on commercial terms. During 1994 we have worked on two systems. One was installed at FTU in Frascati. The other system is for RFX in Padova and was made ready for shipment by the end of the year.

4.1.1 Construction of Multishot Pellet Injectors for FTU, Frascati, and RFX, Padova

(H. Sørensen, B. Sass, K-V. Weisberg, and J. Bundgaard (Engineering and Computer Department, Risø))

The multishot pellet injector delivered to FTU in November 1993 was set up at FTU by the FTU staff in April-May 1994. It was used for injection of pellets until July when FTU was closed down for major maintenance.

The injector for RFX should have been delivered in May 1994 but the delivery was postponed to coincide with a large shutdown. It is now planned that this shutdown will take place in January-April 1995 and delivery must then take place during this period.

The two injectors are similar in design.

Eight pellets of hydrogen or deuterium are made simultaneously and fired successively. They pass through a diagnostic unit where mass and velocity are measured. They continue to the experiment through a guide tube system. They pass two large vacuum chambers where most of the driver gas is removed.

There are, however, differences that made the building and commissioning of the RFX injector more difficult. The main differences are: longer flight distance for pellets for the RFX injector before entering the experiment; larger pellets and, thus, larger gun barrel diameters; stronger cooling needed because of larger pellets; pellets of three different sizes in the RFX injector and only two in the FTU injector; for RFX pellets should be fired with time intervals around 10 ms, for FTU around 100 ms; in the torus hall the cables and tubes between the injector cubicle with instruments and the injector had to be around 12 m at RFX against 2 m at FTU.

The larger effective distance between cubicle and injector meant that the methods for change of pressurised cylinders for pellet gas had to be improved to avoid contamination of pellet gas.

The firing accuracy must then be largest for the RFX injector. In fact, the pellets must be well inside a 25 mm circle 3500 mm in front of the gun barrels.

The gun barrels are very close to each other. When pellets are fired with small time intervals, the flight of a pellet may be affected by driver gas leaving the

neighbour barrel after the preceding shot. In the RFX injector the pellets are fired in the succession large-small-large-small etc. and the firing accuracy of the smaller pellets may then be affected.

The RFX injector must then fire more accurately and at the same time some of the pellets are more inaccurate. This was solved by using the same technique as in the feasibility study made earlier. Here the pellet trajectories were held together by sending the pellets through a 16 mm tube during the last part of their flight. This tube thus acted as a guide tube for some pellets. The same technique was used during test of the RFX injector. A 1,500 mm long tube of 16 mm inside diameter ending around 3,300 mm in front of the gun barrels was mounted and lined up very precisely. An optical detector was set up after this tube and connected to an electronic counter.

It is then possible to check that the same number of pellets is registered by the counter and the diagnostic unit. The pellets hit an aluminium plate of 0.3 mm thickness placed after the 16 mm tube and it is then also possible to see how much the pellets scatter.

Using this method with the aluminium plate placed 3,900 mm in front of the gun barrels, all pellets were inside a 17-20 mm circle for high and low velocity pellets of both hydrogen and deuterium.

For deuterium pellets high velocities are around 1,250-1,300 m/s and low velocities around 730-780 m/s. For hydrogen high velocities are around 1,400-1,450 m/s and low velocities around 800-900 m/s. Velocities vary from one barrel to the other. Scatter in velocity for the individual barrels is around 0.5-2.0%.

For both hydrogen and deuterium the nominal pellet sizes are $1.5 \cdot 10^{20}$, $3 \cdot 10^{20}$, and $5 \cdot 10^{20}$ atoms/pellet. There are four small pellets and two of each of the larger ones. The true pellet size for a barrel may differ up to 6-7% for the nominal one. For each barrel the standard deviation for the scatter in mass is around 2-6%.

5 Publications and Educational Activities

5.1 Optics

5.1.1 Publications

Andersen, A.W.; Christensen, S.S.; Jørgensen, T.M., An active vision system for robot guidance using a low cost neural network board. In: Proceedings. EURISCON '94. Vol. 1: Stream A. European robotics and intelligent systems conference, Malaga (ES), 22-25 Aug 1994. (AMARC. University of Bristol, Bristol, 1994) p. 480-488.

Andersen, A.W.; Christensen, S.S.; Jørgensen, T.M.; Liisberg, C., An active vision system for robot guidance using a low cost neural network board. In: Machine vision applications, architectures, and systems integration 3. Conference on machine vision applications, architectures, and systems integration 3, Boston, MA (US), 31 Oct - 2 Nov 1994. Batchelor, B.G.; Snell Solomon, S.; Waltz, F.M. (eds.), (The International Society for Optical Engineering, Bellingham, WA, 1994) (SPIE Proceedings, 2347) p. 163-170.

Andersen, P.E.; Petersen, P.M.; Buchhave, P., Multiple grating interactions in photorefractive optical interconnects. In: Conference on lasers and electro-optics Europe. CLEO/Europe '94, Amsterdam (NL), 28 Aug - 2 Sep 1994. (The Institute of Electrical and Electronics Engineers, Piscataway, NJ, 1994) p. 65-66.

Andersen, P.E.; Petersen, P.M.; Buchhave, P., Crosstalk in photorefractive optical

interconnects due to nonlinear mixing of gratings. Opt. Photonics News (1994), v. 5 (no. 12) p. 11-12.

Andersen, P.E.; Petersen, P.M.; Buchhave, P., Crosstalk in dynamic optical interconnects in photorefractive crystals. Appl. Phys. Lett. (1994) v. 65 p. 271-273.

Atar, D.; Ramanujam, P.S.; Saunamki, K.; Haunsø, S., Assessment of coronary artery stenosis pressure gradient by quantitative coronary arteriography in patients with coronary artery disease. Clin. Physiol. (1994) v. 14 p. 23-35

Churnside, J.H.; Hanson, S.G., Effect of penetration depth and swell-generated tilt on delta-k lidar performance. Appl. Opt. (1994) v. 33 p. 2363-2368.

Dutkiewicz, L.; Pedrys, R.; Schou, J., Sputtering by excimer production from solid krypton. Europhys. Lett. (1994) v. 27 p. 323-328.

Edvold, B.; Andersen, P.E.; Buchhave, P.; Petersen, P.M., Polarization properties of a photorefractive $Bi_{12}SiO_{20}$ crystal and their application in an optical correlator. IEEE J. Quantum Electron. (1994) v. 30 p. 1075-1089.

Ellegaard, O.; Schou, J.; Stenum, B.; Sørensen, H.; Pedrys, R.; Warczak, B.; Oostra, D.J.; Haring, A.; Vries, A.E. de, Sputtering of solid nitrogen and oxygen by keV hydrogen ions. Surf. Sci. (1994) v. 302 p. 371-384.

Glückstad, J.; Martini Jørgensen, T., Optoelectronic loop that implements a mean field annealing algorithm for nonlinear noise filtering. Opt. Eng. (1994) v. 33 p. 1206-1213.

Glückstad, J.; Ramanujam, P.S., Array illuminator based on transverse self-phase modulation in bacteriorhodopsin thin film. In: LEOS '94. Conference proceedings. Vol. 2. IEEE Lasers and Elctro-Optics Society 1994 annual meeting, Boston, MA (US), 31 Oct - 3 Nov 1994. (Institute of Electrical and Electronics Engineers, New York, 1994) p. 318-319.

Hanson, S.G.; Churnside, J.H.; Wilson, J.J., Remote sensing of wind velocity and strength of refractive turbulence using a two-spatial-filter receiver. Appl. Opt. (1994) v. 33 p. 5859-5868.

Hanson, S.G.; Hansen, B.H., Laser-based measurement scheme for rotational measurement of specularly reflective shafts. In: Fiber optic and laser sensors 12. Conference on fiber optic and laser sensors, San Diego, CA (US), 25-27 Jul 1994. (The International Society for Optical Engineering, Bellingham, WA, 1994) (SPIE Proceedings, 2292) p. 143-153.

Hanson, S.G.; Lindvold, L.R., High accuracy sensor for dynamic measurements based on holographic optical elements, semiconductor lasers and detectors. In: Conference on lasers and electro-optics Europe. CLEO/Europe '94, Amsterdam (NL), 28 Aug - 2 Sep 1994. (The Institute of Electrical and Electronics Engineers, Piscataway, NJ, 1994) p. 68-69.

Hanson, S.G.; Lading, L.; Michelsen, P.; Skaarup, B. (eds.), Optics and Fluid Dynamics Department annual progress report for 1993. Risø-R-715(EN) (1994) 58 p.

Hanson, S.; Zavorotny, V., Multipath scattering of microwaves from the ocean surface. Lawrence Livermore National Laboratory. Workshop on scattering from rough surfaces at low grazing angles (LGA) of incidence, Livermore, CA (US), 26-27 May 1994, p. 144.

Johansen, P.M.B., Two-wave mixing with externally applied magnetic field and Faraday effect on photorefractive medium. IEEE J. Quantum Electron. (1994) v. 30 p. 1916-1923.

Jørgensen, T.M.; Christensen, S.S.; Andersen, A.W.; Liisberg, C., Optimization and application of a RAM based neural network for fast image processing tasks. In: Intelligent robots and computer vision 8: Algorithms and computer vision. Conference on intelligent robots and computer vision 8: Algorithms and computer vision, Boston, MA (US), 31 Oct - 2 Nov 1994. Casasent, D.P. (ed.), (The International Society for Optical Engineering, Bellingham, WA, 1994)

(SPIE Proceedings, 2353) p. 328-338.

Kulinna, C.; Zebger, I.; Hvilsted, S.; Ramanujam, P.S.; Siesler, H.W., Characterization of the segmental mobility of liquid-crystalline side-chain polyesters by Fourier-Transform infrared spectroscopy. Macromol. Symp. (1994) v. 83 p. 169-181.

Kulinna, C.; Zebger, I.; Siesler, H.W.; Hvilsted, S.; Ramanujam, P.S., Characterisation of the orientational behaviour of liquid-crystalline side-chain polymers for reversible optical data storage by Fourier-Transform-IR-Spectroscopy. In: Fourier transform spectrosocpy. 9. International conference on Fourier transform spectroscopy, Bertie, J.E.; Wieser, H. (eds.), (The International Society for Optical Engineering, Bellingham, WA, 1993) (SPIE Proceedings, 2089) p. 476-477.

Lading, L., Principles of laser anemometry. In: Optical diagnostics for flow processes. Lading, L.; Wigley, G.; Buchhave, P. (eds.), (Plenum Press, New York, 1994) p. 85-126.

Lading, L.; Edwards, R.V.; Hanson, S., A phase screen approach to collective light scattering; Resolving temporal fluctuations. In: Seventh international symposium on applications of laser techniques to fluid mechanics. Vol. 1. 7. International symposium on applications of laser techniques to fluid mechanics, Lisbon (PT), 11-14 July 1994. (The Calouste Gulbenkian Foundation, Lisbon, 1994) p. 1.1.1-1.1.6.

Lading, L.; Wigley, G.; Buchhave, P. (eds.), Optical diagnostics for flow processes. (Plenum Press, New York, 1994) 398 p.

Lindvold, L.; Imam, H.; Ramanujam, P.S., Bacteriorhodopsin: A holographic material assessment. POPAM ESPRIT project 6863. (Risø National Laboratory. Optics and Fluid Dynamics Department, Roskilde, 1994) 23 p.

Lindvold, L.R.; Imam, I.; Ramanujam, P.S., The sensitometric properties of chemically modified bacteriorhodopsin films. In: Optical memory. International conference on optical memory and neural networks, Moscow (RU), 27-30 Aug 1994. Mikaelian, A.I. (ed.), (The International Society for Optical Engineering, Bellingham, WA, 1994) (SPIE Proceedings, 2429) p. 22-33.

Martini Jørgensen, T.; Glückstad, J., Diffraction from a wavelet point of view: Comment. Opt. Lett. (1994) v. 19 p. 423.

Martini Jørgensen, T.; Glückstad, J., Q-state mean field annealing algorithm for filtering of grey level images suited for optoelectronic implementation. In: Neural and stochastic methods in image and signal processing 3. Conference on neural and stochastic methods in image and signal processing 3, San Diego, CA (US), 28-29 Jul 1994. Su-Shing Chen (ed.), (The International Society for Optical Engineering, Bellingham, WA, 1994) (SPIE Proceedings, 2304) p. 246-252.

Pedersen, H.C.; Johansen, P.M., Observation of misalignment of the subharmonic grating in photorefractive $Bi_{12}SiO_{20}$. In: Conference on lasers and electro-optics Europe. CLEO/Europe '94, Amsterdam (NL), 28 Aug - 2 Sep 1994. (The Institute of Electrical and Electronics Engineers, Piscataway, NJ, 1994) p. 84-85.

Pedersen, H.C.; Johansen, P.M., Observation of angularly tilted subharmonic gratings in photorefractive bismuth silicon oxide. Opt. Lett. (1994) v. 19 p. 1418-1420.

Pedersen, H.C.; Johansen, P.M., Observation af nye subharmoniske gitre i fotorefractive medier. DOPS-nyt (1994) v. 9 (no.4) p. 10.

Petersen, P.M., Optical phase conjugation and optical signal processing in photorefractive materials. In: Studies in classical and quantum nonlinear optics. 5. International Topsøe summer school on nonlinear optics, Aalborg (DK), 3-8 Aug 1992. Keller, O. (ed.), (Nova Science Publishers, Commack, NY, 1994)

Paper 13.

Petersen, P.M.; Skettrup, T., Ulineær optik. (Polyteknisk Forlag, Lyngby, 1994) 224 p.

Ramanujam, P.S.; Glückstad, J.; Lindvold, L.R.; Rasmussen, J.J., Dynamic contrast reversal due to self-phase modulation in bacteriorhodopsin thin film. Opt. Mem. Neural Networks (1994) v. 3 p. 321-327.

Rohleder, H.; Petersen, P.M.; Marrakchi, A., Quantitative measurement of the vibrational amplitude and phase in photorefractive time-average interferometry: A comparison with electronic speckle pattern interferometry. J. Appl. Phys. (1994) v. 76 p. 81-84.

Saffman, M., Dynamisk optisk informationsbehandling i fotorefraktive kredsløb. DOPS-nyt (1994) v. 9 (no. 4) p. 15-20.

Schou, J., Sputtering of frozen gases by ion and electron bombardment. In: SACSP 94. Symposium on atomic, cluster and surface physics. Contributions. Symposium on atomic, cluster and surface physics, Hintermoos/Maria Alm (AT), 20-26 Mar 1994. Märk, T.D.; Schrittwieser, R.; Smith, D. (eds.), (Institut für Ionenphysik. Universität Innsbruck, Innsbruck, 1994) p. 72-75.

Skov Jensen, A.; Rasmussen, E.; Eilertsen, E.; Sobolev, A.G.; Volkov, V.; Reitblat, G.; Vasiliev, A.A., Processing of temporal or spatial optical flows with acousto-optic correlators. In: Advances in optical information processing 6. 6. Conference on advances in optical information processing, Orlando, FL (US), 6-7 Apr 1994. Pape, D.R. (ed.), (SPIE, Bellingham, 1994) (SPIE Proceedings Series, 2240) p. 83-94.

Smirnov, A.; Drobysh, P.; Jensen, A.; Rasmussen, E.; Pozhidaev, E.; Belyaev, V., Active matrix liquid crystal reflective double-SLM for a joint transform correlator. In: Conference record of the 1994 international display research conference. 1994 International display research conference, Monterey, CA (US), 10-13 Oct 1994. (Society for Information Display, Los Angeles, CA, 1994) p. 257-258.

Sobolev, A.G.; Volkov, V.A.; Kvasha, M.Y.; Dadeshidze, V.V.; Kompanets, I.N.; Vasiliev, A.A.; Epikhin, E.E.; Skov Jensen, A.; Rasmussen, E.; Eilertsen, E., Time-integrating hybrid waveguide acousto-optic correlator. Risø-R-738(EN) (1994) 26 p.

Stenum, B.; Schou, J.; Gürtler, P., UV luminescence of NeD in solid neon-deuterium mixtures. Chem. Phys. Lett. (1994) v. 229 p. 353-356.

Svendsen, W.; O'Sullivan, G., Statistics and characteristics of xuv transition arrays from laser-produced plasmas of the elements tin through iodine. Phys. Rev. A (1994) v. 50 p. 3710-3718.

Thestrup, B.; Svendsen, W.; Schou, J.; Ellegaard, O., Sputtering of thick deuterium films by keV electrons. Phys. Rev. Lett. (1994) v. 73 p. 1444-1447.

5.1.2 Unpublished Contributions

Anderson, D.Z.; Zozulya, A.; Montemezzani, G.; Zhou, G.; Saffman, M., Acoustic signal processing with photorefractive neural networks. 10. Interdisciplinary laser science conference. Optical Society of America annual meeting, Dallas, TX (US), 2-7 Oct 1994. Unpublished. Abstract available.

Baragiola, R.A.; Dukes, C.A.; Schou, J.; Ritzau, S., Plasmon-assisted electron emission from Al and Mg surfaces. Conference of the interaction of charged particles and radiation with matter, Oak Ridge, TN (US), 23-25 Oct 1994. Unpublished. Abstract available.

Buchhave, P.; Andersen, P.E.; Petersen, P.M., Nonlinear combinations of gratings in BSO. Dansk Optisk Selskab Årsmøde 1994. DTU, Lyngby (DK), 24 Nov

1994. Unpublished. Abstract available.

Dam-Hansen, C., Current aspects of laser induced gratings. Fysisk Instituts Optikgruppe, DTH, Risø (DK), 28 Jan 1994. Unpublished.

Dam-Hansen, C.; Johansen, P.M.; Petersen, P.M., Properties of laser induced gratings in lithium niobate crystals. Laser '94. Dansk Optisk Selskab. Dansk Fysisk Selskab, Odense (DK), 12-13 Apr 1994. Unpublished. Abstract available.

Dam-Hansen, C., Fourier transforming properties of lenses, applications. Ph.d.-kursus i moderne fysik. DTU, Lyngby (DK), 19 Apr 1994. Unpublished.

Dam-Hansen, C., Interference filters in photorefractives. Topical meeting on diffractive optics. Danish Optical Society, Risø (DK), 11 Oct 1994. Unpublished.

Dam-Hansen, C., Photorefractive interference filters. Ph.d.-kursus i optik. DTU, Lyngby (DK), 10 Nov 1994. Unpublished.

Dutkiewicz, L.; Pedrys, R.; Schou, J., Particle dynamics during electronic sputtering of solid krypton. 6. International workshop on desorption induced by electronic transitions, Krakow (PL), 26-29 Sep 1994. Unpublished. Abstract available.

Ellegaard, O.; Schou, J.; Svendsen, W., Laser-induced evaporation yields of metallic systems evaluated by numerical methods. Gordon conference on laser interactions with surfaces, New London, NH (US), 15-19 Aug 1994. Unpublished. Abstract available.

Hanson, S.G., Radar backscattering fra havoverflader: Polarimetriske effekter. Forsvarets Forskningstjeneste, København (DK), 26 Jan 1994. Unpublished.

Hanson, S., Multiple scattering effects at low grazing angle. Environmental Technology Laboratory ocean sensing review, Boulder, CO (US), 23 May 1994. Unpublished.

Hanson, S.G., Enhanced radar backscatter at grazing angles. US-Norway ocean radar program 1994. Informal planning session, yer (NO), 9-12 Jan 1994. Unpublished.

Hanson, S.G., White light interferometry: Measurement of optical turbulence. Laser '94. Dansk Optisk Selskab. Dansk Fysisk Selskab, Odense (DK), 12-13 Apr 1994. Unpublished. Abstract available.

Hanson, S.G.; Hurup Hansen, B., Måling af udbøjninger ved anvendelse af differentiel elektronisk Speckle interferometri. Eksperimentel mekanikdag 1994. Aalborg Universitetscenter, Aalborg (DK), 16 Mar 1994. Unpublished. Abstract available.

Hanson, S.G.; Hurup Hansen, B., Measurement of rotational speed based on speckle correlation. Dansk Optisk Selskab Årsmøde 1994. DTU, Lyngby (DK), 24 Nov 1994. Unpublished. Abstract available.

Hvilsted, S.; Pedersen, M.; Ramanujam, P.S.; Andruzzi, F., Erasable optical storage in azobenzene side-chain polyesters. In: EPF 94. Abstract book. 5. European Polymer Federation symposium on polymeric materials, Basel (CH), 9-12 Oct 1994. (European Polymer Federation, Basel, 1994) IT 05.

Johansen, P.M., Photorefractive interference filters. Institut d'Optique Thorique et Applique, Paris (FR), 29 Jun 1994. Unpublished.

Johansen, P.M., Nonlinear excitations of space-charge waves in photorefractive media. Institut d'Optique Théorique et Applique, Paris (FR), 29 Jun 1994. Unpublished.

Johansen, P.M., Photorefractive interference filters. Universidad de Cadiz, Cadiz (ES), 10 Oct 1994. Unpublished.

Johansen, P.M., Z-scan technique for measuring N2. Universidad de Cadiz, Cadiz (ES), 10 Oct 1994. Unpublished.

Johansen, P.M., Observation of misalignment of the subharmonic grating in photorefractive $Bi_{12}SiO_{20}$. Universidad de Cadiz, Cadiz (ES), 10 Oct 1994. Un-

published.

Johansen, P.M., Photorefractive interference filters. Universidad Autonoma de Madrid, Madrid (ES), 11 Oct 1994. Unpublished.

Johansen, P.M., Subharmonic generation in BSO. Universidad Autonoma de Madrid, Madrid (ES), 11 Oct 1994. Unpublished.

Lading, L.; Coherent light scattering. In: W7-X Diagnostic-Working Session, Garching (G), 3 March 1994. Unpublished.

Lading, L.; Edwards, R.V., A phase screen approach to collective light scattering. Aussis (F), 21-24 March 1994. Unpublished.

Lading, L.; Edwards, R.V., A phase screen approach to collective light scattering. Laser '94. Dansk Optisk Selskab. Dansk Fysisk Selskab, Odense (DK), 12-13 Apr 1994. Unpublished. Abstract available.

Lading, L.; Martini Jørgensen, T., Detection and estimation in quantum limited light scattering systems, or how to make the best use of photons. Laser '94. Dansk Optisk Selskab. Dansk Fysisk Selskab, Odense (DK), 12-13 Apr 1994. Unpublished. Abstract available.

Lindvold, L.R.; Imam, H.; Ramanujam, P.S., Spatial frequency response and transient anisotropy of bacteriorhodopsin thin films. In: Frontiers in information optics. Topical meeting of the International Commission for Optics, Kyoto (JP), 4-8 Apr 1994. (ICO, Kyoto, 1994) p. 277.

Meyer, W.V.; Tin, P.; Mann, Jr., J.A.; Cheung, H.M.; Rogers, R.B.; Lading, L., A preview of a modular surface light scattering instrument with autotracking optics. In: International Symposium on Space Optics, April 18-22, Garmisch-Partenkirchen (A), EOS/SPIE Joint Venture, paper 2210-29. Unpublished.

Pedersen, H., Subharmonics in photorefractive materials and wave propagation in anisotropic media. Ph.D.-vejledere fra DTH og Risø, Risø (DK), 28 Jan 1994. Unpublished.

Pedersen, H.C.; Johansen, P.M., Nonlinear two-wave mixing by anisotropic grating diffraction in photorefractive BSO. Laser '94. Dansk Optisk Selskab. Dansk Fysisk Selskab, Odense (DK), 12-13 Apr 1994. Unpublished. Abstract available.

Pedersen, H., Thick volume gratings. Ph.d.-kursus i moderne fysik. DTU, Lyngby (DK), 19 Apr 1994. Unpublished.

Pedersen, M.; Hvilsted, S.; Andruzzi, F.; Ramanujam, P.S., New side-chain liquid crystalline polyesters for optical storage. In: Nordiske polymerdage 1994. Programme and abstracts. Nordiske polymerdage 1994, Copenhagen (DK), 30 May - 1 Jun 1994. (H.C. Ørsted Institute, Copenhagen, 1994) Paper P.6.

Petersen, P.M., Optical processing with photorefractive crystals. Technische Hochschule. Institute of Applied Physics, Darmstadt (DE), 17-19 Aug 1994. Unpublished.

Petersen, P.M., Nonlinear interactions between gratings in photorefractive crystals. Technische Hochschule. Institute of Applied Physics, Darmstadt (DE), 17-19 Aug 1994. Unpublished.

Petersen, P.M., Four-wave mixing in solid. Universidad de Cadiz, Cadiz (ES), 8-10 Oct 1994. Unpublished.

Petersen, P.M., Amplitude and phase measurements in photorefractive time average interferometry. Universidad de Cadiz, Cadiz (ES), 8-10 Oct 1994. Unpublished.

Petersen, P.M., Nonlinear grating interaction in photorefractive materials. Universidad Autonomia, Madrid (ES), 8-10 Oct 1994. Unpublished.

Petersen, P.M.; Hanson, S.G., Photorefractive time-average interferometry and holographic optical elements for industrial sensors. BRITE-EURAM. Technical University of Denmark, Lyngby (DK), 7 Sep 1994. Unpublished.

Ramanujam, P.S.; Andruzzi, F.; Hvilsted, S., Influence of the length of flexi-

ble spacers on the optical storage properties of side-chain liquid crystalline polyesters. In: Frontiers in information optics. Topical meeting of the International Commission for Optics, Kyoto (JP), 4-8 Apr 1994. (ICO, Kyoto, 1994) p. 176.

Saffman, M.; Zozulya, A.A., Propagation of light beams in photorefractive media: Fanning, self-bending and phase conjugation. Danish Physical Society spring meeting, Odense (DK), 2-3 Jun 1994. Unpublished. Abstract available.

Schou, J., Dynamics of rigid bodies. University of Virginia, Charlottesville, VA (US), 14 Oct 1994. Unpublished.

Schou, J., Ion-surface scattering. Vanderbilt University. Department of Physics and Astronomy, Nashville, TN (US), 26 Oct 1994. Unpublished.

Schou, J.; Stenum, B.; Ellegaard, O.; Pedrys, R.; Dutkiewicz, L., Sputtering of the most volatile solids: The solid hydrogens. 10. Inelastic ion surface collisions conference, Grand Targhee, WY (US), 8-12 Aug 1994. Unpublished. Abstract available.

Shi, M.; Westley, M.S.; Baragiola, R.A.; Schou, J.; Johnson, R.E., Satellite and ring atmospheres produced by ion, electron and photo-sputtering of icy sateilites and ring particles: Laboratory measurements. 6. International conference on laboratory research for planetary atmospheres, Bethesda, MD (US), 30 Oct 1994. Unpublished. Abstract available.

Skov Jensen, A., Decoding of PIV images and investigation of hardware realisations. NASA LEWIS Center, Cleveland, OH (US), 30 Mar 1994. Unpublished. Abstract available.

Skov Jensen, A., Decoding of PIV images and investigation of hardware realisations. Carnegie-Mellon University. Department of Electrical and Computer Engineering, Pittsburg, PA (US), 1 Apr 1994. Unpublished. Abstract available.

Skov Jensen, A.; Rasmussen, E.; Eilertsen, E.; Sobolev, A.G.; Volkov, V.; Reitblat, G.; Vasiliev, A., Machine stereo vision based on local correlations. Case Western Reserve University. Electrical Engineering Department, Cleveland, OH (US), 31 Mar 1994. Unpublished. Abstract available.

Skov Jensen, A.; Rasmussen, E.; Eilertsen, E.; Sobolev, A.G.; Volkov, V.; Reitblat, G.; Vasiliev, A., Machine stereo vision system based on local correlations. Carnegie-Mellon University. Department of Electrical and Computer Engineering, Pittsburgh, PA (US), 1 Apr 1994. Unpublished. Abstract available.

Svendsen, W., Laser ablation from Silver. Lecture at Risø National Laboratory, Roskilde (DK), February 1994. Unpublished.

Svendsen, W., Diffraction. Lecture at Ørsted Laboratory, Niels Bohr Institute, Copenhagen (DK), 3 November 1994. Unpublished.

Svendsen, W., Laser ablation, Hvad er det og hvorfor. Fysik Stjerne Foredrag på Ørsted Laborariet, Niels Bohr Institute, Copenhagen (DK). Unpublished.

Svendsen, W.; Schou, J.; Ellegaard, O., Laser ablation from metallic targets. Laser '94. Dansk Optisk Selskab. Dansk Fysisk Selskab, Odense (DK), 12-13 Apr 1994. Unpublished. Abstract available.

Svendsen, W.; Schou, J.; Ellegaard, O., Laser ablation from silver targets. Danish Physical Society spring meeting, Odense (DK), 2-3 Jun 1994. Unpublished. Abstract available.

Svendsen, W.; Schou, J.; Thestrup, B., Laser ablation from metals. Gordon conference on laser interactions with surfaces, New London, NH (US), 15-19 Aug 1994. Unpublished. Abstract available.

Svendsen, W.; Thestrup, B.; Schou, J.; Ellegaard, O., Sputtering of thin and intermediately thick films of solid deuterium by keV electrons. 6. International workshop on desorption induced by electronic transitions, Krakow (PL), 26-29 Sep 1994. Unpublished. Abstract available

Thestrup Nielsen, B., Sputtering of solid D2 by keV electrons: Dependence of

yield on film thickness. Danish Sputtering Club, Risø (DK), 24 Feb 1994. Unpublished.

Thestrup, B.; Svendsen, W.; Schou, J.; Ellegaard, O., Erosion of solid deuterium of various film thicknesses by keV electrons. Danish Physical Society spring meeting, Odense (DK), 2-3 Jun 1994. Unpublished. Abstract available.

Zebger, I.; Siesler, H.W.; Andruzzi, F.; Pedersen, M.; Ramanujam, P.S.; Hvilsted, S., The influence of substituents on the orientational behaviour of novel azobenzene side-chain polyesters. In: 11th European symposium on polymer spectroscopy. ESOPS-11. Programme. Book of abstracts. 11. European symposium on polymer spectroscopy, Valladolid (ES), 20-22 Jul 1994. (University of Valladolid, Valladolid, 1994) p. 86

5.2 Continuum Physics

5.2.1 Publications

Astradsson, L.; Jensen, V.O. (eds.), Annual progress report 1993. Work in controlled thermonuclear fusion research performed in the fusion research unit under the contract af association between Euratom and Risø National Laboratory. Risø-R-761(EN) (1994) 50 p.

Bang, O.; Juul Rasmussen, J.; Christiansen, P.L., Subcritical localization in the discrete nonlinear Schrödinger equation with arbitrary power nonlinearity. Nonlinearity (1994) v. 7 p. 205-218.

Coutsias, E.A.; Bergeron, K.; Lynov, J.P.; Nielsen, A.H., Self organization in 2D circular shear layers. In: 25th AIAA plasmadynamics and lasers conference. 25. AIAA plasmadynamics and lasers conference, Colorado Springs, CO (US), 20-23 Jun 1994. (American Institute of Aeronautics and Astronautics, Washington, DC, 1994) (AIAA-94-2407) 11 p.

Hanson, S.G.; Lading, L.; Michelsen, P.; Skaarup, B. (eds.), Optics and Fluid Dynamics Department annual progress report for 1993. Risø-R-715(EN) (1994) 58 p.

Hesthaven, J.S.; Gottlieb, D., A stable penalty method for the compressible Navier-Stokes equations. I. Open boundary conditions. (Institute for Computer Applications in Science and Engineering. NASA Langley Research Center, Hampton, VA, 1994) (NASA-CR-194961; ICASE-R-94-68) 41 p.

Karpman, V.I.; Lynov, J.P.; Michelsen, P.K.; Juul Rasmussen, J., Modulational instability evolution in two dimensions. In: 1994 International conference on plasma physics. Proceedings. Contributed papers. Vol. 2. 10. Kiev international conference on plasma theory; 10. International congress on waves and instabilities in plasmas; 6. Latin American workshop on plasma physics, Foz do Iguacu, PR (BR), 31 Oct - 4 Nov 1994. Sakanaka, P.H.; Bosco, E. Del; Alves, M.V. (eds.), (INPE/Setor de Eventos, Sao Jos dos Campos, SP, 1994) p. 71-74.

Jensen, V.O., Alfvenbølger. Den store Danske Encycklopædi, Danmarks Nationalleksikon, vol. I, p. 249, 1994.

Jensen, V.O., Fusion. Ungdommens Naturvidenskabelige Forening. UNF, København (DK), 1 Sep 1994. Unpublished. Abstract available.

Karpman, V.I.; Lynov, J.P.; Michelsen, P.K.; Juul Rasmussen, J., Modulational instability of plasma waves in two dimensions. In: Computational physics nonlinear dynamical phenomena in physical, chemical and biological systems. 3. IMACS international conference on computational physics, Lyngby (DK), 1-4 Aug 1994. Leth Christiansen, P.; Mosekilde, E. (eds.), (IMACS Secretariat. Department of Computer Science. Rutgers University, Piscataway, NJ, 1994)

p. 113-118.

Lynov, J.P.; Coutsias, E.A.; Hesthaven, J.S., New spectral algorithms for accurate simulations of bounded flows. In: Advanced concepts and techniques in thermal modelling. Oral and poster communications extended papers. EUROTHERM seminar 36, Poitiers (FR), 21-23 Sep 1994. (Laboratoire d'Etudes Thermiques, Poitiers, 1994) p. N16-N21.

Lynov, J.P.; Hesthaven, J.S.; Juul Rasmussen, J.; Nycander, J.; Sutyrin, G.G.; Shirshov, P.P., Coherent structure in anisotropic plasmas. In: 25th AIAA plasmadynamics and lasers conference. 25. AIAA plasmadynamics and lasers conference, Colorado Springs, CO (US), 20-23 Jun 1994. (American Institute of Aeronautics and Astronautics, Washington, DC, 1994) (AIAA-94-2408) 8 p.

Lynov, J.P.; Michelsen, P.K.; Juul Rasmussen, J., Investigations of etai-vortices. In: 1994 International conference on plasma physics. Proceedings. Contributed papers. Vol. 2. 10. Kiev international conference on plasma theory; 10. International congress on waves and instabilities in plasmas; 6. Latin American workshop on plasma physics, Foz do Iguacu, PR (BR), 31 Oct - 4 Nov 1994. Sakanaka, P.H.; Bosco, E. Del; Alves, M.V. (eds.), (INPE/Setor de Eventos, Sao Jos dos Campos, SP, 1994) p. 91-94.

Nielsen, A.H.; Lynov, J.P.; Coutsias, E.A.; Bergeron, K., Self organization in 2D circular shear layers. In: Computational physics nonlinear dynamical phenomena in physical, chemical and biological systems. 3. IMACS international conference on computational physics, Lyngby (DK), 1-4 Aug 1994. Leth Christiansen, P.; Mosekilde, E. (eds.), (IMACS Secretariat. Department of Computer Science. Rutgers University, Piscataway, NJ, 1994) p. 119-124.

Nielsen, A.H.; Pécseli, H.L.; Juul Rasmussen, J., Experimental evidence for mode selection in turbulent plasma transport. Europhys. Lett. (1994) v. 27 p. 209-214.

Raadu, M.A.; Rasmussen, J.J.; Turitsyn, S.K., Stability of small-amplitude double layers in a two-temperature plasma. Plasma Phys. Rep. (1993) v. 19 p. 531-536.

Ramanujam, P.S.; Glückstad, J.; Lindvold, L.R.; Rasmussen, J.J., Dynamic contrast reversal due to self-phase modulation in bacteriorhodopsin thin film. Opt. Mem. Neural Networks (1994) v. 3 p. 321-327.

Rasmussen, J. Juul; Hesthaven, J.S.; Lynov, J.P.; Nielsen, A.H.; Schmidt, M.R., Dipolar vortices in two-dimensional flows. (Invited contribution). In: Computational physics nonlinear dynamical phenomena in physical, chemical and biological systems. 3. IMACS international conference on computational physics, Lyngby (DK), 1-4 Aug 1994. Leth Christiansen, P.; Mosekilde, E. (eds.), (IMACS Secretariat. Department of Computer Science. Rutgers University, Piscataway, NJ, 1994) p. 1-11.

Rasmussen, J. Juul; Stenum, B., Visualization of coherent structures. In: Optical diagnostics for flow processes. Lading, L.; Wigley, G.; Buchhave, P. (eds.), (Plenum Press, New York, 1994) p. 291-302.

Rasmussen, J. Juul; Lynov, J.P.; Hesthaven, J.S.; Sutyrin, G.G., Vortex dynamics in plasmas and fluids. Plasma Phys. Controlled Fusion (1994) v. 36 p. B193-B202.

Sutyrin, G.G.; Hesthaven, J.S.; Lynov, J.P.; Juul Rasmussen, J., Dynamical properties of vortical structures on the beta-plane. J. Fluid Mech. (1994) v. 268 p. 103-131.

Sønderberg Petersen, L.; Jensen, V.O., Drømmen om en uudtømmelig energikilde er rykket nærmere virkeligheden. Risø nyt (1994) (no. 3) p. 10-11.

Sønderberg Petersen, L.; Jensen, V.O., Drømmen om en uudtømmelig energikilde er rykket nærmere virkeligheden. DaFFO-nyt. Dansk Forening til Fremme af Opfindelser (1994) v. 22 (no. 6) p. 6-11.

5.2.2 Unpublished Contributions

Hesthaven, J.S., The penalty method for systems of hyperbolic and mixed type (invited lecture). In: Spectral Multi-Domain Workshop, Rayleight, North Carolina (US), 18-21 May 1994. Unpublished.

Hesthaven, J.S., A penalty method for problems in fluid mechanics. In: Workshop on Spectral Methods, The Technical University of Denmark, Lyngby (DK), 27 May 1994. Unpublished.

Hesthaven, J.S., Penalty methods for spectral methods. Lecture at University of New Mexico, Department of Mathematics and Statistics, Albuquerque (US). Unpublished.

Hesthaven, J.S.; Lynov, J.P.; Nielsen, A.H.; Rasmussen, J.J.; Schmidt, M.R.; Shapiro, E.G.; Turitsyn, S.K., Dynamics of nonlinear dipole vortices. European Geophysical Society 19. general assembly, Grenoble (FR), 25-29 Apr 1994. Unpublished. Abstract available.

Hesthaven, J.S.; Lynov, J.P.; Nielsen, A.H.; Juul Rasmussen, J.; Schmidt, M.R., Dynamics of nonlinear dipole vortices. Danish Physical Society spring meeting, Odense (DK), 2-3 Jun 1994. Unpublished. Abstract available.

Hesthaven, J.S., No-slip boundary conditions for the 2D Navier-Stokes equations in the $\omega - \psi$ formulation. Lecture at Brown University, Division of Applied Mathematics Providence, Rhode Island (US), 11 February 1994. Unpublished.

Jensen, V.O., Fusionsplasmafysik. Forelæsningsserie. Danmarks Tekniske Universitet, Lyngby (DK), September-December 1994. Unpublished. Lecture notes available.

Jensen, V.O., Magnetic stresses in ideal MHD. 29. Nordic plasma and gas discharge symposium, Geilo (NO), 31 Jan - 2 Feb 1994. Unpublished. Abstract available.

Jensen, V.O., Magnetiske spændinger i statiske magnetfelter. Afdelingen for Elektrofysik. DTU, Lyngby (DK), 24 Jan 1994. Unpublished. Abstract available.

Jensen, V.O., Fusionsenergien, Fremtidens uudtømmelige energikilde. Plancher vist på Danmarks Tekniske Museum under energi udstilling, juni - December 1994.

Jensen, V.O., Fusionsenergien, fremtidens uudtømmelige og miljøvenlige energikilde. Fællesseminar for VUC-centrene i København (DK), 30 november 1994. Unpublished.

Kuznetsov, E.A.; Rasmussen, J.J., Instability of two-dimensional solitons and vortices in a defocucing media. International workshop on nonlinear Schroedinger equation: Achievements, developments, perspectives (NLS-94), Chernogolovka, Moscow Region (RU), 25 Jul - 3 Aug 1994. Unpublished. Abstract available.

Kuznetsov, E.A.; Rasmussen, J.J.; Rypdal, K.; Turitsyn, S.K., Sharper criteria for the wave collapse. (Invited contribution). International workshop on nonlinear Schroedinger equation: Achievements, developments, perspectives (NLS-94), Chernogolovka, Moscow Region (RU), 25 Jul - 3 Aug 1994. Unpublished. Abstract available

Lynov, J.P.; Bergeron, K.; Coutsias, E.A.; Nielsen, A.H., Evolution of circular shear layers. In: 1994 IEEE international conference on plasma science. IEEE conference record - abstracts. 1994 IEEE international conference on plasma science, Santa Fe, NM (US), 6-8 Jun 1994. (Institute of Electrical and Electronics Engineers, New York, 1994) p. 81-82.

Lynov, J.P., Accurate Determination of no-slip solvability constraints. Department

of Mathematics and Statistics, University of New Mexico, Albuquerque (US), 18 May 1994. Unpublished.

Lynov, J.P., Full-wave calculations of the O-X mode conversion in magnetized plasmas. Department of Mathematics and Statistics, University of New Mexico, Albuquerque (US), 22 February 1994. Unpublished.

Lynov, J.P., Two-dimensional dipole interactions with straight and curved walls. Department of Mathematics and Statistics, University of New Mexico, Albuquerque (US), 4 May 1994. Unpublished.

Michelsen, P.K., Vortices in η_i–modes. In: Transport in Fusion Plasmas, Aspenäs, Göteborg (S), 13-16 June 1994. Unpublished.

Michelsen, P.K., Two lectures 1) Fusion Energy and 2) Plasma Transport and drift wave instabilities. H.C. Ørsted Institute, Copenhagen (DK), 5 May 1994. Unpublished.

Michelsen, P.K.; Karpman, V.I.; Lynov, J.P.; Juul Rasmussen, J., Modulational instability of plasma waves in two dimensions. Danish Physical Society spring meeting, Odense (DK), 2-3 Jun 1994. Unpublished. Abstract available.

Nielsen, A.H.; Pécseli, H.L.; Rasmussen, J. Juul, Experimental investigations of turbulent transport in the edge plasma of the Q-machine. (Invited contribution). In: The 29 Nordic Plasma and Gas Discharge Symposium, Geilo (N), 31 January - 2 February 1994. Unpublished.

Rasmussen, J. Juul, Vortex dynamics in plasmas and fluids. (Invited contribution). In: 21st EPS conference on controlled fusion and plasma physics. Abstracts of invited and contributed papers. 21. EPS conference on controlled fusion and plasma physics, Montpellier (FR), 27 Jun - 1 Jul 1994. Joffrin, E.; Platz, P.; Stott, P.E. (eds.), (The European Physical Society, Montpellier, 1994) p. 17

Rasmussen, J. Juul, Vortical structures in plasmas and fluids. Institute seminar, Chalmers University of Technology, Institute for Electromagnetic Field Theory and Plasma Physics, Gothenburg (S), 11 January 1994. Unpublished.

Rasmussen, J. Juul, Coherent structures in plasmas and fluids. (Invited contribution). In: 1994 International Conference on Plasma Physics, Foz do Iguacu, PR (Brazil), 31 October - 4 November 1994. Unpublished.

Saffman, M.; Lading, L., A hybrid doppler/time-of-flight laser anemometer for turbulence measurements in a magnetized fusion plasma. Lecture at Max Planck Institut für Plasma Physik, Garching (D), 8 November 1994. Unpublished.

Sutyrin, G.G.; Yushina, I.G.; Hesthaven, J.S.; Lynov, J.P.; Rasmussen, J.J., Nonlinear interaction between a monopolar vortex and its Rossby wave wake. (Invited contribution). European Geophysical Society 19. general assembly, Grenoble (FR), 25-29 Apr 1994. Unpublished. Abstract available.

6 Personnel

Scientific Staff

Christensen, Steen Sloth
Gervang, Bo
Hanson, Steen Grüner
Jensen, Arne Skov
Jensen, Vagn O.
Johansen, Per Michael
Jørgensen, Thomas Martini
Kristensen, Jesper Glückstad (from 1 October)
Lading, Lars
Laursen, Thorkild S. (from 1 March)
Lindvold, Lars R.
Lynov, Jens-Peter
Michelsen, Poul K.
Nielsen, Anders H.
Petersen, Paul Michael
Ramanujam, P.S.
Rasmussen, Jens Juul
Saffman, Mark (from 1 April)
Schou, Jørgen
Stenum, Bjarne
Sørensen, Hans
Weisberg, Knud-V. (until 31 October)

Ph.D. Students

Dam-Hansen, Carsten
Hesthaven, Jan S.
Holme, Niels Chr. R.
Kristensen, Jesper Glückstad (until 30 September)
Pedersen, Henrik C.
Schmidt, Michel R. (from 1 October)
Svendsen, Winnie E.

Technical Staff

Bækmark, Lars
Eilertsen, Erik
Hansen, Bengt Hurup
Hansen, Bent Skov (from 8 August)
Michelsen, Agnete (until 30 April)
Moustgaard, Stig (until 25 June)
Nielsen, Mogens O.
Nordskov, Arne
Rasmussen, Erling
Reher, Børge
Sass, Bjarne
Søefeldt, Allan E. (until 25 June)
Stubager, Jørgen
Thorsen, Jess

Secretaries

Astradsson, Lone
Jensen, Elin
Skaarup, Bitten (from 15 December)
Toubro, Lene

Guest Scientists

Bergé, Luc, Commisariat á l'Energie Atomique, Centre d'Etudes de Limeil-Valenton, France
Fridken, Vladimir, Institute of Crystallography, Moscow, Russia
He, Xingyu, University of Warwick, Coventry, England
Imam, Husein, King's College London, England
Mezentsew, Vladimir, Institute of Automation and Electrometry, Russian Academy of Sciences, Novosibirsk, Russia
Snezhkin, E.N., Russian Research Center Kurchatov Institute, Moscow, Russia
Sturman, Boris I., Institute of Automation and Electrometry, Russian Academy of Sciences, Novosibirsk, Russia
Wyller, John, Narvik Institute of Technology, Norway
Yura, Hal, Aerospace Corporation, USA

Short-term Visitors

Pécseli, H.L., University of Oslo, Norway
Sutyrin, G.G., P.P. Shirshov Institute of Oceanology, Moscow, Russia
Luther, G.G., University of New Mexico, Albuquerque, USA
Scott, B.D., Max-Planck-Institut für Plasmaphysik, Garching, Germany
Van Heijst, G.J., Technical University of Eindhoven, The Netherlands
McCluskey, D, Dantec Measurement Technology A/S, Skovlunde, Denmark
Høst Madsen A., Dantec Measurement Technology A/S, Skovlunde, Denmark

Students Working for the Master's Degree

de Nijs, Robin
Hansen, René Skov
Nielsen, Birgitte T.
Pedersen, Thomas Sunn
Rezei, Mac

Student Assistants

Okkels, Fridolin, (August 1 - September 15)
Schmidt, Michel R. (January 17-28 and September 19 - October 1)

Bibliographic Data Sheet **Risø-R-793(EN)**

Title and author(s)

Optics and Fluid Dynamics Department
Annual Progress Report for 1994

S.G. Hanson, L. Lading, J.P. Lynov, and P. Michelsen

ISBN	ISSN
87-550-2044-5	0106-2840 0906-1797

Dept. or group	Date
Optics and Fluid Dynamics Department	January 1995

Groups own reg. number(s)	Project/contract No.

Pages	Tables	Illustrations	References
68		27	44

Abstract (Max. 2000 char.)

Research in the Optics and Fluid Dynamics Department is performed within the following two programme areas: optics and continuum physics. In optics the activities are within (a) optical materials and electromagnetic propagation, (b) diagnostics and sensors, and (c) information processing. In continuum physics the activities are (a) nonlinear dynamics and (b) computer physics. The activities are supported by several EU programmes, including EURATOM, by research councils, and by industry. A special activity is the implementation of pellet injectors for fusion research. A summary of activities in 1994 is presented.

Descriptors INIS/EDB

DYNAMICS; FLUIDS; LASERS; NONLINEAR OPTICS; NONLINEAR PROBLEMS; NUMERICAL SOLUTION; PLASMA; PROGRESS REPORT; RESEARCH PROGRAMS; RISOE NATIONAL LABORATORY; THERMONUCLEAR REACTIONS

Available on request from:
Risø Library, Risø National Laboratory (Risø Bibliotek, Forskningscenter Risø)
P.O. Box 49, DK-4000 Roskilde, Denmark
Phone (+45) 46 77 46 77, ext. 4004/4005 · Telex 43 116 · Fax (+45) 46 75 56 27

RISØ

Objective

The objective of Risø's research is to provide industry and society with new potential in three main areas:

- *Energy technology and energy planning*
- *Environmental aspects of energy, industrial and plant production*
- *Materials and measuring techniques for industry*

As a special obligation Risø maintains and extends the knowledge required to advise the authorities on nuclear matters.

Research Profile

Risø's research is long-term and knowledge-oriented and directed toward areas where there are recognised needs for new solutions in Danish society. The programme areas are:

- *Combustion and gasification*
- *Wind energy*
- *Energy technologies for the future*
- *Energy planning*
- *Environmental aspects of energy and industrial production*
- *Environmental aspects of plant production*
- *Nuclear safety and radiation protection*
- *Materials with new physical and chemical properties*
- *Structural materials*
- *Optical measurement techniques and information processing*

Transfer of Knowledge

The results of Risø's research are transferred to industry and authorities through:

- *Research co-operation*
- *Co-operation in R&D consortia*
- *R&D clubs and exchange of researchers*
- *Centre for Advanced Technology*
- *Patenting and licencing activities*

To the scientific world through:

- *Publication activities*
- *Co-operation in national and international networks*
- *PhD- and Post Doc. education*

Key Figures

Risø has a staff of just over 900, of which more than 300 are scientists and 80 are PhD and Post Doc. students. Risø's 1995 budget totals DKK 476m, of which 45% come from research programmes and commercial contracts, while the remainder is covered by government appropriations.

Risø-R-793(EN)
ISBN 87-550-2044-5
ISSN 0106-2840
ISSN 0906-1797

Available on request from:
Risø Library
Risø National Laboratory
P.O. Box 49, DK-4000 Roskilde, Denmark
Phone +45 46 77 46 77, ext. 4004/4005
Telex 43116, Fax +45 46 75 56 27